



Published in final edited form as:

*Acta Physiol (Oxf)*. 2019 April ; 225(4): e13213. doi:10.1111/apha.13213.

## Neurons in the rat ventral lateral preoptic area are essential for the warm-evoked inhibition of brown adipose tissue and shivering thermogenesis

Ellen P. S. Conceição, Christopher J. Madden, Shaun F. Morrison

Department of Neurological Surgery, Oregon Health & Science University, Portland, Oregon

### Abstract

**Aim:** To determine the role of neurons in the ventral part of the lateral preoptic area (vLPO) in CNS thermoregulation.

**Methods:** In vivo electrophysiological and neuropharmacological were used to evaluate the contribution of neurons in the vLPO to the regulation of brown adipose tissue (BAT) thermogenesis and muscle shivering in urethane/chloralose-anaesthetized rats.

**Results:** Nanoinjections of NMDA targeting the medial preoptic area (MPA) and the vLPO suppressed the cold-evoked BAT sympathetic activity (SNA), reduced the BAT temperature ( $T_{BAT}$ ), expired  $CO_2$ , mean arterial pressure (MAP), and heart rate. Inhibition of vLPO neurons with muscimol or AP5/CNQX elicited increases in BAT SNA,  $T_{BAT}$ , tachycardia, and small elevations in MAP. The BAT thermogenesis evoked by AP5/CNQX in vLPO was inhibited by the activation of MPA neurons. The inhibition of BAT SNA by vLPO neurons does not require a GABAergic input to dorsomedial hypothalamus (DMH), but MPA provides a GABAergic input to DMH. The activation of vLPO neurons inhibits the BAT thermogenesis evoked by NMDA in the rostral raphe pallidus (rRPa), but not that after bicuculline in rRPa. The BAT thermogenesis elicited by vLPO inhibition is dependent on glutamatergic inputs to DMH and rRPa, but these excitatory inputs do not arise from MnPO neurons. The activation of neurons in the vLPO also inhibits cold- and prostaglandin-evoked muscle shivering, and vLPO inhibition is sufficient to evoke shivering.

**Conclusion:** The vLPO contains neurons that are required for the warm ambient-evoked inhibition of muscle shivering and of BAT thermogenesis, mediated through a direct or indirect GABAergic input to rRPa from vLPO.

### Keywords

dorsomedial hypothalamus; fever; medial preoptic area; rostral raphe pallidus; shivering; thermoregulation

---

**Correspondence** Ellen P. S. da Conceição, Department of Neurological Surgery, Oregon Health & Science University, Portland, OR. santosda@ohsu.edu.

CONFLICT OF INTEREST

No conflicts of interest, financial or otherwise are declared by the authors.

## 1 | INTRODUCTION

The maintenance of an appropriate core body temperature (TCORE) is critical for life. Severe hypothermia or hyperthermia impairs cellular function and disrupts homeostasis. The preoptic area (POA) of the hypothalamus is an important locus for integrating the cutaneous, CNS, and body core thermal signalling to control thermoeffector activity in response to environmental or immune challenges. POA neurons can influence TCORE through the sympathetic regulation of brown adipose tissue (BAT) thermogenesis<sup>1</sup> and cutaneous vasoconstriction,<sup>2</sup> and through the activation of muscle shivering<sup>3</sup> and thermodefensive behaviours.<sup>4,5</sup> Preoptic area neurons project to the dorsomedial hypothalamus (DMH) and to the rostral raphe pallidus (rRPa)<sup>6</sup> to influence the activity of thermogenesis-promoting and thermogenesis premotor neurons respectively.<sup>7-9</sup> In particular, during warm exposure, inhibitory GABAergic inputs to DMH neurons from the medial preoptic area (MPA),<sup>1,10,11</sup> as well as the ventral medial preoptic area (VMPO), including the median preoptic nucleus (MnPO),<sup>11</sup> are proposed to suppress thermogenesis by reducing the excitatory drive to BAT sympathetic and to shivering somatic premotor neurons in the rRPa.<sup>3,10</sup> The removal of this inhibition during skin cooling increases the activity of thermogenesis-promoting neurons in the DMH which then drives premotor neurons in the rRPa to increase BAT and shivering thermogenesis.

In addition to the MPA and the VMPO, the ventral part of the lateral preoptic area (vLPO) also contributes to the regulation of TCORE. Neurons in the vLPO are infected after the injection of pseudorabies virus into the interscapular BAT,<sup>12,13</sup> they express c-fos after exposure to a warm ambient temperature,<sup>14</sup> and neurotoxic lesions in the LPO impair heat defense,<sup>15</sup> consistent with a potential role for vLPO neurons in suppressing thermogenesis during heat defense. In mice, heat exposure induces c-fos expression in a population of GABAergic neurons in vLPO which project to DMH<sup>16</sup>; and optogenetic activation of these vLPO GABAergic neurons or their terminals in the DMH, reduced “activity thermogenesis” (ie, the heat production generated by increased movement<sup>17,18</sup>) and decreased TCORE.<sup>16</sup>

We undertook the present study to extend our understanding of the role of neurons in the rat vLPO in thermoregulation, specifically with regard to the control of BAT and shivering thermogenesis. In testing the hypothesis that neurons in the vLPO exert an inhibitory influence on BAT thermogenesis and muscle shivering in a warm or thermoneutral environment, we determined that vLPO contains neurons whose tonic activity in the warm maintains a GABAergic inhibition of thermogenesis premotor neurons in the rRPa that is necessary and sufficient to restrict heat production in warm conditions. This discovery reinforces the idea that a warm-activated inhibitory mechanism, rather than the simple absence of a cold thermoreceptor-driven excitation maintains the low level of BAT and shivering thermogenesis in warm environments.

## 2 | RESULTS

### 2.1 | Activation of neurons in rat vLPO or in MPA inhibits BAT thermogenesis

To determine if the BAT sympathoinhibitory responses, or the pathways mediating them, might be different between neurons in MPA and those in the vLPO, we began by observing

the BAT sympathoinhibitory responses to activation of neurons in these two regions of the rat POA (Figure 1A). We used nanoinjections of the glutamatergic agonist, NMDA targeted to activate local neurons in three regions (see Section 14) in the POA (Figure 1B–D), and evaluated their effects on the BAT thermogenic and the cardiovascular responses to skin cooling. Since NMDA is quickly cleared from the synaptic cleft,<sup>19</sup> the diffusion of injectate and its duration of action should be limited.

Unilateral nanoinjections ( $n = 5$ ) of NMDA targeting the rostral region of the HDB (Figure 1B), including two injections that were located more caudally in the dorsal LPO (Figure 1C) had no effect on cold-evoked BAT SNA,  $T_{\text{CORE}}$ , MAP, or HR (Table 1).

Unilateral nanoinjections ( $n = 5$ ) of NMDA targeting the region of the vLPO (Figure 1C,D) completely inhibited cold-evoked BAT SNA, eliciting a reduction of  $-100\% \pm 4\%$  ( $P = 0.04$ ) of the cold-evoked BAT SNA, and resulting in decreases in  $T_{\text{BAT}}$ , Exp  $\text{CO}_2$ , MAP, and HR (Figure 1A, Table 1). The transitory inhibition of BAT thermogenesis did not affect the  $T_{\text{CORE}}$  (Table 1).

Unilateral nanoinjections ( $n = 10$ ) of NMDA targeting the rostral (Figure 1B) or the caudal (Figure 1C,D) regions of the MPA evoked a  $-96\% \pm 6\%$  ( $P = 0.001$ ) reduction in the level of cold-evoked BAT SNA, which caused a decrease in  $T_{\text{BAT}}$  and Exp  $\text{CO}_2$ , accompanied by falls in MAP and HR, but no change in  $T_{\text{CORE}}$  (Figure 1A, Table 1).

Overall, a significant inhibition of BAT thermogenesis, a modest bradycardia and small hypotensive responses can be elicited by activation of POA neurons medially in the rostral and caudal levels of MPA, and laterally at the caudal, but not the rostral, level of the vLPO. In subsequent experiments, we targeted neurons in the vLPO and in the MPA for the further study.

## 2.2 | Activation of GABA<sub>A</sub> receptors in the vLPO elicits BAT thermogenesis

We next sought to determine if the BAT sympathoinhibitory neurons in the vLPO region are tonically active when the rat is warm and there is little or no activity on the sympathetic nerve to BAT. This result would be consistent with BAT sympathoinhibitory neurons in the vLPO region participating in the warm-evoked inhibition of BAT thermogenesis. Under warm conditions, activation of local GABA<sub>A</sub> receptors in the vLPO (Figure 2C,  $n = 8$ ) with bilateral nanoinjections of muscimol (1.2 mmol/L, 60 nL) elicited a large and sustained increase in BAT SNA, resulting in a strong BAT thermogenesis (Figure 2A). The stimulation of BAT SNA (peak:  $+2349\% \pm 1549\%$  BL from a pre-muscimol level of  $172\% \pm 90\%$  BL,  $P = 0.002$ ) produced increases in  $T_{\text{BAT}}$ , Exp  $\text{CO}_2$ , and  $T_{\text{CORE}}$ , accompanied by an elevated MAP and HR (Figure 2A, Table 2). These data indicate that under the warm conditions of our experiment, the BAT sympathoinhibitory neurons in the vLPO area are tonically active and exerting a potent restraining effect on BAT thermogenesis.

## 2.3 | Blockade of glutamate receptors in the vLPO elicits BAT thermogenesis

To determine if a glutamatergic excitatory drive contributes to the tonic activity of BAT sympathoinhibitory neurons in the vLPO area under warm conditions, we nanoinjected (60 nL) a cocktail of the ionotropic glutamate receptor antagonists, AP5 (5 mmol/L) and CNQX

(5 mmol/L) bilaterally into vLPO (Figure 2D,  $n = 6$ ) in warm rats with negligible levels of BAT SNA. Similar to the effect of muscimol injections in the vLPO, AP5/CNQX in vLPO also elicited significant increases in BAT SNA (peak:  $1059\% \pm 725\%$  BL, from a pre-AP5/CNQX level of  $115\% \pm 7\%$  BL,  $P = 0.01$ ), resulting in elevations in  $T_{BAT}$ , Exp  $CO_2$ , and  $T_{CORE}$ , but with no change in MAP or HR (Figure 2B, Table 2).

#### 2.4 | BAT thermogenesis evoked by the blockade of glutamate receptors in the vLPO is inhibited by activation of MPA neurons

Could the BAT sympathoinhibitory effects of activating neurons in the MPA (Figure 1A) be mediated by glutamatergic activation of neurons in the vLPO? The blockade of ionotropic glutamate receptors in the vLPO (Figure 3B) increased BAT SNA and  $T_{BAT}$  (Figure 3A). Subsequent activation of neurons in MPA (Figure 3B,  $n = 4$ ) with nano-injections of NMDA led to a prompt reversal of the increases in BAT thermogenic and cardiovascular variables elicited by glutamate receptor blockade in the vLPO (Figure 3A). The NMDA-stimulated activation of neurons in MPA inhibited BAT SNA  $-100\% \pm 0.4\%$  of the elevated level of  $781\% \pm 106\%$  BL following AP5/CNQX in vLPO ( $P = 0.0005$ ), which reduced  $T_{BAT}$  ( $-0.2 \pm 0.2^\circ C$  from  $36.7 \pm 0.8^\circ C$  following AP5/CNQX in vLPO,  $P = 0.047$ ), Exp  $CO_2$  ( $-0.2\% \pm 0.1\%$  from  $5.3\% \pm 0.6\%$  following AP5/CNQX in vLPO,  $P = 0.03$ ). The activation of neurons in MPA also reversed the small increases in MAP ( $-8 \pm 7$  mm Hg from  $122 \pm 25$  mm Hg following AP5/CNQX in vLPO,  $P = 0.046$ ) and HR ( $-24 \pm 5$  bpm from  $387 \pm 35$  bpm following AP5/CNQX in vLPO,  $P = 0.01$ ), which were evoked by blocking glutamate receptors in the vLPO. The transitory inhibition of BAT thermogenesis did not affect the  $T_{CORE}$  ( $-0.01 \pm 0.1^\circ C$  from  $37.9 \pm 0.8^\circ C$  following AP5/CNQX in vLPO,  $P = 0.4$ ). These results indicate that the BAT sympathoinhibitory effects of activating neurons in the MPA are not mediated by a glutamatergic activation of neurons in the vLPO. Thus, these results argue against a serial connection between neurons in MPA and vLPO, but rather provide support for the hypothesis that the BAT sympathoinhibitory effects of activating neurons in the MPA and in the vLPO are mediated via different circuit mechanisms.

#### 2.5 | Neurons in the MPA, but not those in the vLPO, require GABA<sub>A</sub> receptor activation in the DMH to inhibit BAT thermogenesis

The findings that the MPA contains GABAergic neurons projecting to the DMH neurons that provide an input to neurons in the rRPa<sup>20</sup> and that activation of GABAergic projections from the mouse vLPO to DMH causes hypothermia<sup>16</sup> is consistent with the possibility that the inhibitions of BAT thermogenesis elicited from these two regions of the POA are mediated similarly by a GABAergic inhibition of thermogenesis-promoting neurons in the DMH. To test the role of GABA<sub>A</sub> receptor-mediated inhibition of DMH neurons in the inhibition of BAT SNA elicited from the rat MPA and from the rat vLPO, we observed the effect of activating the neurons in each of these two areas after bilateral nano-injections of BIC into the DMH. The disinhibition of neurons in the DMH with nano-injections of BIC (1 mmol/L, 60 nL) elicits a significant increase in BAT SNA and BAT thermogenesis.<sup>21</sup>

Unilateral activation with NMDA of neurons in either the left or right vLPO (Figure 4B,  $n = 4$ ) reversed the elevated BAT SNA evoked by the bilateral disinhibition of neurons in DMH (Figure 4A,B), but a similar activation of neurons in the MPA (Figure 4D,  $n = 5$ ) had no

effect on the elevated BAT thermogenesis following bilateral BIC in DMH (Figure 4C,D). NMDA in vLPO reduced the DMH disinhibition-evoked level of BAT SNA by  $-96\% \pm 6\%$  ( $P = 0.04$ ), as well the TBAT, Exp CO<sub>2</sub>, MAP, and HR (Table 3). This transitory inhibition of the BAT thermogenesis did not impact the T<sub>CORE</sub>. In contrast, after blocking GABA<sub>A</sub> receptors in the DMH, activation of neurons in the MPA had no effect on BAT SNA, T<sub>CORE</sub>, MAP, or HR (Table 3). The dependence of the BAT sympathoinhibitory effectiveness of neurons in the MPA on GABA<sub>A</sub> receptors in the DMH is consistent with current models<sup>3,8</sup> suggesting a GABAergic input from the MPA to the DMH in the thermoregulatory control of BAT SNA. The finding that the inhibition of BAT SNA evoked from the vLPO does not require a GABAergic input to DMH provides a clear distinction between the pathways mediating the BAT sympathoinhibitory effects from these two POA regions.

## 2.6 | Activation of vLPO neurons inhibits the BAT thermogenesis evoked by NMDA in rRPa, but not that after BIC in rRPa

Although BIC injection in the rRPa of warm rats elicits large and sustained increases in BAT SNA and BAT thermogenesis,<sup>22</sup> the source of the relevant, tonically active GABAergic input to rRPa is unknown. Since inhibition of the activity of vLPO neurons also elicits large increases in BAT SNA (Figure 2), we tested whether a GABAergic input to rRPa is required for the BAT sympathoinhibition evoked from activating neurons in vLPO.

After the nanoinjection of BIC (1 mmol/L, 60 nL) in rRPa (Figure 5C,  $n = 5$ ), nanoinjection of NMDA into the vLPO bilaterally had no effect on the elevated levels of BAT SNA, T<sub>BAT</sub>, Exp CO<sub>2</sub>, and T<sub>CORE</sub> evoked by rRPa disinhibition (Figure 5A, Table 4). However, the activation of neurons in the vLPO reduced the elevated MAP and HR (Table 4).

In contrast, unilateral activation of neurons in either the left or right vLPO completely reversed the stimulation of BAT SNA and BAT thermogenesis evoked by nanoinjections of NMDA (0.2 mmol/L, 60 nL) in the rRPa (Figure 5B,D,  $n = 5$ ). NMDA in vLPO reduced BAT SNA by  $-97\% \pm 5\%$  ( $P = 0.01$ ) from the level evoked by glutamatergic activation of rRPa neurons, decreased T<sub>BAT</sub>, Exp CO<sub>2</sub>, MAP, and HR, with no effect on the T<sub>CORE</sub> (Table 4).

## 2.7 | Thermogenesis elicited by vLPO inhibition is dependent on a glutamatergic input to DMH

A glutamatergic output from the MnPO to the DMH has been proposed to mediate a BAT sympathoexcitatory effect.<sup>23–25</sup> We tested the potential role of a MnPO-derived glutamatergic input to the DMH in the BAT sympathoexcitation following inhibition of neurons in the vLPO (see Figure 2A). Under a warm condition, bilateral nanoinjections of muscimol in vLPO (Figure 6B) elicited large increases in BAT SNA and BAT thermogenesis (Figure 6A). Bilateral nanoinjections (60 nL each) of AP5/CNQX (5 mmol/L each) in the DMH (Figure 6B,  $n = 4$ ) terminated the elevation in BAT SNA evoked by inhibition of neurons bilaterally in the vLPO (Figure 6A), resulting in a  $-98\% \pm 3\%$  ( $P = 0.01$ ) fall in BAT SNA (Table 5) from the level following inhibition of vLPO neurons. The elevations in T<sub>BAT</sub>, Exp CO<sub>2</sub>, T<sub>CORE</sub>, MAP, and HR were also significantly reduced (Table 5). In contrast, inhibition of local neurons in the MnPO (Figure 6D) with single nanoinjections of muscimol

(1.2 mmol/L, 60 nL, n = 4) had no effect on the elevated level of BAT SNA and BAT thermogenesis following GABAergic inhibition of neurons in the vLPO (Figure 6C, Table 5); in fact,  $T_{BAT}$  and  $T_{CORE}$  continued to rise after muscimol injection in the MnPO (Table 5). These results suggest that neurons in the MnPO region we targeted with muscimol are not the source of the glutamatergic excitatory input to the DMH that mediates the activation of BAT thermogenesis following inhibition of neurons in the vLPO.

## 2.8 | Thermogenesis elicited by vLPO inhibition is dependent on a glutamatergic input to rRPa

The rRPa contains sympathoexcitatory premotor neurons that activate BAT thermogenesis<sup>10</sup> and HR,<sup>26,27</sup> and are necessary for the sympathetic responses to stimulation of neurons in the DMH and in the POA.<sup>2,3,28–31</sup> The rRPa also contains somatic premotor neurons required for the activation of skeletal muscle shivering.<sup>3,32</sup> We examined the involvement of a glutamatergic input to neurons in the rRPa in the BAT thermogenesis evoked by inhibition of neurons in vLPO.

After bilateral nanoinjections of muscimol in the vLPO (Figure 7A,B) under warm conditions, nanoinjection (60 nL) of AP5/CNQX (5 mmol/L each) in the rRPa (n = 4) caused an immediate cessation of BAT SNA, resulting in a reduction in the vLPO inhibition-evoked level of  $-101\% \pm 3\%$  ( $P = 0.00003$ ) from the vLPO inhibition-evoked level of  $1167\% \pm 474\%$  BL, and decreasing  $T_{BAT}$  ( $-1.2 \pm 1.0^{\circ}\text{C}$  from  $38.3 \pm 0.9^{\circ}\text{C}$ ,  $P = 0.049$ ), Exp  $\text{CO}_2$  ( $-0.9\% \pm 0.4\%$  from  $5.9\% \pm 1.3\%$ ,  $P = 0.01$ ),  $T_{CORE}$  ( $-0.1 \pm 0.1^{\circ}\text{C}$  from  $38.4 \pm 0.9^{\circ}\text{C}$ ,  $P = 0.04$ ), MAP ( $-17 \pm 11$  mm Hg from  $124 \pm 22$  mm Hg,  $P = 0.03$ ), and HR ( $-74 \pm 50$  bpm from  $432 \pm 56$  bpm,  $P = 0.03$ ).

## 2.9 | Activation of neurons in the vLPO inhibits cold- and PGE<sub>2</sub>-evoked muscle shivering

Skeletal muscle shivering plays an important role in body temperature regulation, by generating heat in response to skin cooling challenges and during the febrile state.<sup>3</sup> Since the neuroanatomical pathway controlling shivering thermogenesis relies on the POA, DMH, and rRPa<sup>3,33</sup> in a manner paralleling that controlling BAT thermogenesis, we sought to determine if neurons in the vLPO might exert an inhibitory influence on muscle shivering that also parallels their effects on BAT thermogenesis.

Similar to the effect on BAT thermogenesis (Figure 1A), the activation of neurons in the vLPO (n = 6) with nanoinjections of NMDA (0.2 mmol/L, 60 nL) inhibited the muscle shivering elicited by rapid skin cooling (Figure 8A,D, Table 6). NMDA in vLPO reduced cooling-evoked shivering EMG amplitudes in masseter ( $-100\% \pm 0.5\%$ ,  $P = 0.02$ ), nuchal ( $-98\% \pm 3\%$ ,  $P = 0.02$ ), and forelimb ( $-88\% \pm 30\%$ ,  $P = 0.01$ ) muscles, with accompanying reductions in  $T_{BAT}$ , Exp  $\text{CO}_2$ , and HR (Figure 8A, Table 6).

Nanoinjection of PGE<sub>2</sub> in MPA activates local EP3 receptors to produce a febrile state which includes the activation of muscle shivering.<sup>3</sup> Nanoinjections of NMDA (0.2 mmol/L, 60 nL) in the vLPO (n = 4) inhibited the muscle shivering elicited by PGE<sub>2</sub> injections in the MPA (Figure 8B,D). NMDA in vLPO reduced PGE<sub>2</sub>-evoked shivering EMG amplitudes in masseter ( $-96\% \pm 7\%$ ,  $P = 0.03$ ), nuchal ( $-97\% \pm 7\%$ ,  $P = 0.007$ ), and forelimb ( $-93\%$

$\pm 10\%$ ,  $P=0.03$ ) muscles, with accompanying reductions in  $T_{BAT}$ , Exp  $CO_2$ , and HR (Figure 8B, Table 6).

### 2.10 | Inhibition of vLPO evokes muscle shivering

The activity of neurons in the vLPO exerts a brake on the level of BAT thermogenesis (Figures 2, 6, 7). If vLPO neurons are also providing a significant tonic inhibition of muscle shivering under warm conditions, then reducing their activity could elicit spontaneous shivering in the absence of skin cooling. Under warm conditions, with no basal shivering EMG activity (Table 6), activation of local GABA<sub>A</sub> receptors in the vLPO ( $n=4$ ) with bilateral nanoinjections of muscimol (1.2 mmol/L, 60 nL) elicited large and sustained increases in the masseter muscle shivering EMGs (Figure 8C,D):  $+1975\% \pm 1065\%$  ( $P=0.02$ ) in the masseter muscles,  $+1715\% \pm 1101\%$  ( $P=0.03$ ) in the nuchal muscles, and  $+530\% \pm 354\%$  ( $P=0.03$ ) in the forelimb muscles. Shivering was accompanied by increases in  $T_{BAT}$ , Exp  $CO_2$ , and HR (Figure 8C, Table 6).

## 3 | DISCUSSION

The principal finding of our study is that there is a population of thermogenesis-inhibiting neurons within the rat vLPO whose tonic activity is required to maintain the very low levels of BAT thermogenesis and muscle shivering that are observed in thermoneutral or warm ambient conditions. Under warm conditions, inhibition of the activity of neurons in the vLPO results in dramatic increases in BAT SNA, BAT thermogenesis, shivering EMGs, and HR. This BAT activation is supported by glutamatergic excitations of neurons in the DMH and in the rRPa. Increasing the activity of these vLPO neurons completely reverses the increases in BAT SNA and BAT thermogenesis and in muscle shivering that are reflexively evoked by skin/core cooling, and the shivering EMGs during the febrile response to PGE<sub>2</sub> in the POA. In the rat, cooling and PGE<sub>2</sub> in POA also evoke increases in arterial pressure and HR, and these cardiovascular responses are reversed by stimulation of vLPO neurons. The BAT sympathoinhibition mediated by the activation of neurons in the vLPO requires GABA release in the rRPa. This study provides significant new insights into the neural circuit (Figure 9) and neurotransmitter mechanisms through which a population of vLPO neurons provides an important inhibitory regulation of BAT and shivering thermogenesis. In particular, the activity of these vLPO neurons drives a GABAergic input to rRPa that is essential for the inhibition of BAT and shivering thermogenesis that restricts heat production in a warm environment. This discovery emphasizes the concept that the low level of BAT and shivering thermogenesis in a warm environment is mediated by a warm-activated inhibitory mechanism, rather than being due simply to the absence of a cold thermoreceptor-driven excitation of thermogenesis.

This and other functional studies of the thermoregulatory role of POA neurons now support the existence of two populations of GABAergic POA neurons that inhibit thermogenesis. The first, broadly distributed in the MPA, and perhaps in the rostral VMPO,<sup>11</sup> are GABAergic neurons, some of which may be warm-sensitive or expressing the EP3 receptor, that project to the DMH to reduce the discharge of thermogenesis-promoting neurons.<sup>1,11,20</sup> In the present study, we also found that the sympathoinhibition of BAT thermogenesis

following NMDA-mediated activation of neurons in the MPA requires GABA<sub>A</sub> receptors in the DMH. A second population of DMH-projecting GABAergic neurons has recently been identified in the mouse vLPO.<sup>16</sup> Activation of these neurons reduces T<sub>CORE</sub> and “activity thermogenesis” in mice; and inhibition of these neurons leads to significant elevations in T<sub>CORE</sub>.<sup>16</sup> By directly measuring the activity of thermogenic effectors, our data significantly extend the results in mice by demonstrating that activation of neurons in the rat vLPO inhibited cold-evoked BAT SNA and BAT thermogenesis, and inhibited cold- and PGE<sub>2</sub>-evoked shivering. Further, the increases in T<sub>CORE</sub> following inhibition of vLPO neurons in warm rats are mediated through activation of BAT thermogenesis and shivering.

The BAT sympathoinhibition elicited by activating neurons in the rat vLPO was indistinguishable from that similarly evoked from neurons in the rat MPA (Figure 1). However, the BAT sympathoinhibition evoked from the rat vLPO is produced by a different circuit mechanism from that evoked from the MPA since the BAT sympathoinhibition evoked from the rat vLPO requires a direct, or indirect, activation of GABA<sub>A</sub> receptors in the rRPa, while the MPA-evoked sympathoinhibition requires GABA<sub>A</sub> receptor activation in the DMH (Figure 4). The MPA-evoked inhibition of BAT SNA in rats does not occur via a glutamatergic activation of vLPO neurons, since blockade of glutamate receptors in the vLPO did not prevent the inhibition of BAT SNA following activation of MPA neurons (Figure 3). We expect that increasing the activity of neurons in MPA increases GABA release onto neurons in the DMH (Figure 4), whose increased neural discharge is required for the activation of BAT SNA following inhibition of vLPO neuronal activity (Figure 6B).

Since the reductions in T<sub>CORE</sub> and “activity thermogenesis” elicited from optogenetic activation of mouse vLPO neurons are mimicked by similar activation of their GABAergic terminals in DMH, a GABAergic inhibition of thermogenesis-promoting neurons in the DMH was proposed to mediate the thermogenesis-inhibiting effects of activating mouse vLPO neurons.<sup>16</sup> This result would appear to differ from our finding that the BAT sympathoinhibition evoked from the rat vLPO requires a GABAergic input to rRPa (Figure 5). There is strong evidence for a serial, excitatory connection between thermogenesis-promoting neurons in the DMH and premotor neurons for thermogenesis in the rRPa. The BAT activation evoked by disinhibition of DMH neurons with bicuculline is mediated by increased activity of BAT sympathetic premotor neurons in the rRPa.<sup>31</sup> Additionally, a direct glutamatergic excitation of BAT sympathetic premotor neurons in rRPa by DMH neurons drives the BAT activation and hyperthermia during social defeat stress in rats<sup>34</sup> and during cage exchange stress in mice.<sup>35</sup> Our results (Figure 6B and 7A) are also consistent with a DMH-derived glutamatergic excitation of premotor neurons in the rRPa being responsible for the elevated BAT SNA following inhibition of vLPO neurons. Thus, activation of a GABAergic projection from vLPO neurons solely to thermogenesis premotor neurons in the rRPa would reverse a BAT excitation resulting from an increased activity of DMH neurons (eg, cold-evoked, PGE<sub>2</sub>-evoked or stress-evoked), independent of whether or not there was a simultaneous activation of a vLPO-derived GABAergic input to the DMH. Thus, we cannot distinguish between the possibilities that activating neurons in the vLPO drives (a) a GABAergic input solely to rRPa or (b) simultaneous GABAergic inputs to both rRPa and DMH neurons (Figure 9). Retrograde tracing has provided an anatomical substrate for each of these groups of projection neurons in the vLPO region.<sup>6</sup> It will be of interest to determine



if mouse vLPO neurons project to rRPa and, if so, whether activation of their terminals in rRPa inhibits thermogenesis and reduces  $T_{CORE}$ .

Our results (Figure 4C) indicate that the BAT sympathoinhibition evoked by activating neurons in MPA requires activation of a GABAergic input to DMH (Figure 9). Thus, the thermogenesis-inhibiting pathway attributed to the mouse vLPO<sup>16</sup> appears to be similar to that emanating from the rat MPA. In contrast to our results in rat, however, Zhao, et al reported that activation of GABAergic neurons in the mouse “MPO” did not affect  $T_{CORE}$ .<sup>16</sup> It is unclear why activation of rat MPA neurons elicits a strong inhibition of BAT thermogenesis (Figure 1) that is due to a GABAergic input to the DMH (Figure 4C), but no such thermoregulatory effect occurs in mice. Experimental differences include a more caudal position of the “MPO” laser fibre in the mouse than the location of our MPA injections in the rat, an anaesthetic component in the rat, and the selective targeting of GABAergic neurons in the mouse. Resolution of this difference between the specific activation of mouse MPO GABAergic neurons having no effect on  $T_{CORE}$ , but a general activation of rat MPA neurons with NMDA receptors strongly inhibiting BAT SNA (Figure 1) must await further experimentation.

Our results could contribute to an explanation of the increases in TBAT and  $T_{CORE}$  elicited by midline brain transections between the POA and the DMH.<sup>36–38</sup> Such transections could have increased thermogenesis by severing the axons of GABAergic projection neurons in the vLPO, as well as those in the MPA or VMPO. Similarly, the increases in thermogenesis elicited by brain transections near the pontomedullary junction<sup>21</sup> or by axonal conduction block in the midbrain<sup>39</sup> could interrupt an active, vLPO-derived GABAergic inhibition of thermogenesis premotor neurons in the rRPa. In each of these cases, the source(s) of the active excitatory drives to the DMH and to the rRPa remains unknown, although they are expected to be located caudal to the POA.

A glutamatergic input to thermogenesis-promoting neurons in the DMH is required for the sustained activation of BAT SNA following inhibition of neurons in the vLPO (Figure 6A). The increases in BAT SNA during the febrile response to injection of PGE<sub>2</sub> into the MPA,<sup>30</sup> or in response to stress<sup>34</sup> have a similar requirement for a glutamatergic activation of DMH neurons. Neurons in the MnPO play an important role in activating DMH neurons during cold defense and during PGE<sub>2</sub>-evoked fever. The DMH receives projections from MnPO neurons.<sup>24,40</sup> Our finding that inhibition of neurons in the MnPO did not reverse the increase in BAT SNA during inhibition of vLPO neurons (Figure 6C) argues against MnPO neurons as the source of the required glutamatergic excitation of thermogenesis-promoting neurons in the DMH. Although it is possible that our muscimol nano-injections in MnPO were not sufficiently extensive, or that they inhibited populations of MnPO neurons with opposing effects on BAT thermogenesis, the source of the excitation of DMH neurons, revealed after removal of the vLPO-mediated inhibition of BAT SNA, must await future study (Figure 9).

Since the activity of vLPO neurons is necessary for the restraint of BAT and shivering thermogenesis in thermoneutral or warm environments, or when  $T_{CORE}$  is within or above the thermoneutral zone, we would expect that vLPO neurons receive a cutaneous warm thermoreceptor-responsive excitatory input and/or vLPO neurons are intrinsically warm-

sensitive. We have established that vLPO thermogenesis-inhibiting neurons receive an important glutamatergic excitation (Figure 2B), but the source of the glutamatergic excitation of these vLPO neurons that sustains their activity in a thermoneutral or warm environment, as well as whether this glutamatergic input is modulated by cutaneous and/or central warm signalling remains unknown. If vLPO neurons do receive a warm thermoreceptor driven input, we postulate (Figure 9) that this input would arise from warm-responsive neurons in MnPO that receive an input from neurons in LPBd.<sup>41</sup> Cutaneous warm thermoreceptors activate neurons in the LPBd which project to the MnPO,<sup>41</sup> warm exposure activates glutamatergic neurons in MnPO,<sup>25,42</sup> and vLPO receives projections from MnPO neurons.<sup>40,43</sup> Consistent with vLPO neurons receiving a glutamatergic drive from warm-sensitive POA neurons is the finding that blockade of glutamate receptors in the vLPO prevents the inhibition of BAT SNA and BAT thermogenesis evoked by artificial POA warming.<sup>44</sup> In addition to receiving a warm-responsive excitatory input, some neurons in vLPO may exhibit warm-sensitivity, since the transient receptor potential cation channel, subfamily M, member 2 (TRPM2) is expressed there.<sup>45,46</sup>

However, it is unclear why there appear to be two parallel pathways mediating the warm-evoked inhibition of thermogenesis, one involving GABAergic neurons in the MPA and VMPO that inhibit DMH neurons, and another involving GABAergic neurons in the vLPO that inhibit rRPa neurons. It may be that the GABAergic input to rRPa thermogenesis premotor neurons from neurons in the vLPO is not warm responsive, but rather that the vLPO neurons may simply provide a sufficient level of tonic inhibition that its removal (ie, with nanoinjections of muscimol or AP5/CNQX into vLPO) shifts the balance of excitatory and inhibitory inputs to rRPa premotor neurons in favour of excitation, even in a warm environment (Figure 2). In this regard, inhibition of neuronal activity in vLPO might be similar to the blockade of GABA<sub>A</sub> receptors in rRPa which also elicits a strong activation of BAT SNA and BAT thermogenesis in a warm environment.<sup>22</sup> Whether or not this is the case, it will be important to understand the source of the glutamatergic excitation of these vLPO neurons.

The discovery of this novel population of thermogenesis-inhibiting neurons in the rat vLPO, which may complement that in the mouse,<sup>16</sup> requires modifications (Figure 9) of the current models of central thermoregulatory circuits.<sup>1,7-9</sup> In these models, cutaneous warming excites warm-activated, LPBd neurons projecting to the MnPO,<sup>41</sup> which directly or indirectly increase the activity of GABAergic, potentially warm-sensitive, POA projection neurons, located primarily in the MPA<sup>20</sup> and VMPO<sup>11</sup>, that inhibit thermogenesis-promoting neurons in the DMH. Consistent with this model, we found that activation of neurons in MPA inhibited cold-evoked BAT SNA (Figure 1) in a manner dependent on a GABAergic input to DMH (Figure 4C). However, our results (Figures 2, 8) also indicate that the glutamate receptor-driven activity of neurons in vLPO is required for the sustained inhibition of BAT and shivering thermogenesis in a warm environment. Furthermore, the inhibition of thermogenesis by vLPO neurons is dependent on a GABAergic input to thermogenesis premotor neurons in rRPa (Figure 5). Together, these data support a model (Figure 9) in which a population of GABAergic neurons in vLPO, which may receive a potentially warm-driven, glutamatergic excitation, projects to rRPa, and possibly DMH (see above), to inhibit sympathetic and somatic premotor neurons for BAT and for shivering thermogenesis.

Paralleling the effects on BAT thermogenesis and HR, activation of neurons in the vLPO uniformly inhibited skeletal muscle shivering evoked by cooling and by pyrogenic stimulation (Figure 8). Remarkably, eliminating the activity of vLPO neurons resulted in a dramatic and uniform activation of muscle shivering EMGs (Figure 8C), indicating that the activity of vLPO neurons is necessary to prevent shivering in a warm environment. These results enhance the parallels between the central neural circuit mechanisms controlling thermoregulatory muscle shivering and those for BAT thermogenesis, which include the activation of neurons in the MnPO, as well as thermogenesis-promoting neurons in the DMH, and premotor neurons in the rRPa.<sup>3</sup> As with these neuronal populations, we expect that the population of vLPO neurons controlling shivering is distinct from that controlling BAT thermogenesis. This is based not only on the different spinal targets (ie, ventral horn vs intermediolateral cell column) of the rRPa premotor neurons for shivering and for BAT SNA, but also on the different skin and core temperature thresholds for eliciting muscle shivering vs BAT thermogenesis,<sup>3</sup> such that as skin and core temperatures are lowered, BAT thermogenesis is initiated significantly earlier than shivering EMGs. This was also the case for the activation of thermogenesis upon inhibition of neurons in vLPO: BAT thermogenesis was activated markedly earlier than muscle shivering EMGs (Figure 8C). This result is consistent with distinct subsets of neurons in the vLPO providing direct (or indirect) GABAergic inhibition to the respective populations of premotor neurons for BAT SNA and for muscle shivering in the rRPa, and possibly to the respective populations of thermogenesis-promoting neurons in the DMH.

In rodents, but not in humans, cold defense involves a marked tachycardia, mediated principally by activation of cardiac sympathetic premotor neurons in the rRPa.<sup>26</sup> The role of this tachycardia remains unclear, although an additional source of thermogenesis, or an augmented cardiac output to increase BAT blood flow are possibilities. Neurons in the MPA and in the vLPO can significantly modulate cardiovascular function, suppressing stress-related<sup>47</sup> and cold evoked<sup>10,48</sup> hypertension and tachycardia. Similarly, in our experiments, activation of vLPO neurons reduced the elevated AP and reversed the tachycardia elicited during skin cooling, and inhibition of vLPO neurons caused a prominent tachycardia under thermoneutral/warm condition. Blockade of GABA<sub>A</sub> receptors in DMH did not prevent the reduction in HR evoked by activating neurons in vLPO, in contrast to the marked reduction in the bradycardic effect of activating vLPO neurons after bicuculline in the rRPa. Similar to the effects of vLPO neurons on BAT thermogenesis and shivering, these results are consistent with neurons in vLPO providing an inhibitory modulation of the cardiac sympathetic premotor neurons in the rRPa. The small residual effect of vLPO neurons on HR after blockade of GABA<sub>A</sub> receptors in the rRPa (Figure 5A) may arise from an influence of vLPO neurons on the cardiac sympathetic premotor neurons in the rostral ventrolateral medulla. Thus, in warm or thermoneutral environments, vLPO not only provides a tonic inhibition of BAT thermogenesis and muscle shivering, but also contributes to the suppression of a cardiac thermogenesis, as well as the cardiovascular mechanisms that could affect the distribution heat throughout the body, and the delivery of fuel for the metabolic activity of BAT and muscle during cold-evoked thermogenesis.

In summary, the discovery that the activity of vLPO neurons driving a GABAergic input to rRPa is responsible for the restriction of BAT and shivering thermogenesis in a warm

environment highlights the significance of this heretofore unrecognized central inhibitory mechanism in maintaining a low level of facultative heat production in a warm environment. Our findings suggest that the neural circuitry model for the core thermoregulatory control of thermogenesis (Figure 9) must include a population of GABAergic neurons in vLPO that receive a (potentially warm-driven) glutamatergic excitation and project to rRPa to inhibit sympathetic and somatic premotor neurons for BAT and for shivering thermogenesis. These vLPO neurons may also project to DMH to inhibit thermogenesis-promoting neurons. An important unanswered question remains whether and how a reduction in the activity of thermogenesis-inhibiting neurons in vLPO might play a role in the cold-evoked increases in BAT and shivering thermogenesis. Additionally, since the location of the thermogenesis-inhibiting neurons in the vLPO overlaps that of GABAergic, sleep-promoting neurons in the ventrolateral preoptic nucleus (VLPO),<sup>49,50</sup> it will be of interest to determine if thermogenesis-inhibiting neurons in the vLPO play a role in the reduction in TCORE during sleep.

## 4 | MATERIALS AND METHODS

Thirty-nine male Sprague–Dawley rats (300–510 g from Charles River, Indianapolis, IN, USA) contributed to the present study. The animals were housed with ad libitum access to food and water in a room air-conditioned at 22–23°C with a standard 12 hours light-dark cycle. All procedures conform to the regulations detailed in the *National Institutes of Health Guide for the Care and Use of Laboratory Animals* and were approved by the Animal Care and Use Committee of the Oregon Health and Science University.

### 4.1 | Surgical and experimental procedures for experiments involving the recording of BAT sympathetic nerve activity (SNA)

Rats breathing spontaneously were initially anaesthetized with isoflurane (2%–3% in 100% O<sub>2</sub>). The adequacy of anaesthesia was verified by the lack of motor responses to a strong tail pinch. The femoral artery was cannulated for monitoring mean arterial pressure (MAP) and heart rate (HR). The femoral vein was cannulated for intravenous (iv) administration of anaesthesia (urethane, 750 mg/kg iv  $\alpha$ -chloralose, 60 mg/kg iv; both supplemented at 10% of initial dose per hour iv) and neuromuscular blockade (D-tubocurarine, 0.6 mg per rat iv, supplemented with 0.3 mg/hour iv). The adequacy of anaesthesia was assessed hourly and verified by the lack of cardiovascular or motor responses to a strong tail pinch before the neuromuscular blockade. The trachea was cannulated for artificial ventilation with 100% O<sub>2</sub> at a minute volume of 180–240 mL, such that the resting end-expired CO<sub>2</sub> remained between 3.5% and 5.0%. The rats were positioned prone in a stereotaxic frame, in a flat-skull position with the incisor bar at –4 mm below interaural zero. A water-perfused thermal blanket consisting of a silicon sheet with embedded silicon tubing was wrapped completely around the rat's shaved trunk from the shoulders to the hips. The primary purpose of the thermal blanket was to cool the skin (perfusion water temperature: ~20°C), thereby stimulating cutaneous thermoreceptors and eliciting increases in BAT SNA and BAT thermogenesis.<sup>10,51,52</sup> Thermocouples (Physitemp, Clifton, NJ, USA) were inserted into the rectum to measure core body temperature (T<sub>CORE</sub>), into the left interscapular BAT pad to measure BAT temperature (T<sub>BAT</sub>), and onto the flank skin under the thermal blanket to measure skin

temperature ( $T_{\text{SKIN}}$ ) (TC-1000 thermocouple reader, Sable Systems, Las Vegas, NV, USA).  $T_{\text{CORE}}$  was maintained at  $\sim 37.0^{\circ}\text{C}$  with a thermostatically controlled heating lamp, in combination with the water-perfused thermal blanket, except as noted during skin cooling episodes.

#### 4.2 | Surgical and experimental procedures for experiments involving the recording of muscle shivering EMGs

For experiments involving recording of EMGs, the rats were anaesthetized with inactin (120 mg/kg, supplemented with 12 mg/kg/hour). Bipolar needle electrodes for EMG recording were inserted into the nuchal muscle, the forepaw triceps muscle, and the masseter muscle. The EMG signals were filtered (10-1000 Hz) and amplified ( $\times 2000$ ) with a CyberAmp 380 (Axon Instruments, Union City, CA, USA). EMG amplitude was quantified (Spike2, CED, Cambridge, UK) in sequential 4 seconds bins as the square root of the total power (root mean square) in the 0-500 Hz band of the autospectra of each 4 seconds segment of EMG.

#### 4.3 | Administration of drugs

Drugs were administered into brain sites via stereotaxically positioned nanoinjection pipettes (20  $\mu\text{m}$  tip diameter) connected to a pneumatic injection apparatus (Toohey, Fairfield, NJ, USA). The drug nanoinjection volume was 60 nL (estimated using a calibrated microscope reticule to observe the displacement of the fluid meniscus in the glass pipette), with the drug concentration declining over an expected maximum diffusion sphere of approximately 500  $\mu\text{m}$  in diameter.<sup>53</sup>

The rat MPA is centred at 0.7 mm lateral to the midline and the rat LPO is centred at 1.2 mm lateral to the midline.<sup>54</sup> Initially, we targeted three regions (Figure 1B–D): (a) the region of the nucleus of the horizontal limb of the diagonal band (HDB) (+0.1 rostral to bregma, 1.2 mm lateral to the midline, and  $-8.5$  to  $-9.0$  mm below the dural surface), which is located rostral to the vLPO; (b) caudally in the vLPO ( $-0.6$  caudal to bregma, 1.2 mm lateral to the midline, and  $-8.5$  to  $-9.0$  mm below the dural surface); and (c) in the MPA (between +0.1 mm rostral and  $-0.6$  mm caudal to bregma, 0.7 mm lateral to the midline, and  $-8.5$  to  $-9.0$  mm below the dural surface). Other nanoinjections were made in the MnPO (0.0 mm relative to bregma, at the midline, and 6.5-7.0 mm ventral to dura); in the DMH ( $-3.0$  to  $-3.5$  mm caudal to bregma, 0.5-0.7 mm lateral to the midline, and 8.2-9.0 mm ventral to dura); and in the rRPa ( $-12.0$  mm caudal to bregma, at the midline, and 8.5-9.5 mm ventral to dura).

We used N-methyl-D-aspartate (NMDA, 0.2 mmol/L), bicuculline methiodide (BIC, 1 mmol/L), muscimol hydrobromide (1.2 mmol/L), prostaglandin  $E_2$  ( $\text{PGE}_2$ , 1 mg/mL), the NMDA glutamate receptor antagonist, (2R)-amino-5-phosphonovaleric acid (AP5, 5 mmol/L), and the AMPA/kainite glutamate receptor antagonist, 6-cyano-7-nitroquinoxaline-2,3-dione (CNQX, 5 mmol/L). All drugs were obtained from Sigma Aldrich (St. Louis, MO, USA) and dissolved in isotonic saline. Nanoinjection of the isotonic saline vehicle had no effects on either BAT thermogenic or cardiovascular variables.

#### 4.4 | Histological localization of injection sites

The microinjection sites were marked by pressure nanoinjection of fluorescent polystyrene microspheres (Fluo-Spheres, F8797, F8801 or F8803; Molecular Probes, Eugene, OR, USA) included in the injectate (1:100 dilution of FluoSpheres). After the physiological recordings, rats were perfused (5% paraformaldehyde) transcardially, and brains were removed, post-fixed (2-12 hours), and sectioned on a microtome (60  $\mu$ m coronal sections). The sections were mounted on slides, and nanoinjection sites were localized and photographed.

#### 4.5 | Data and statistical analysis

For analysis of BAT SNA, a continuous measure (4 seconds bins) of BAT SNA amplitude was obtained as the root mean square (rms) value of the BAT SNA, calculated (Spike 2, CED) as the square root of the total power in the 0.1-20 Hz frequency band of the autospectra of sequential 4 seconds segments of BAT SNA. To normalize slight differences in nerve recording characteristics among experiments, BAT SNA values are expressed as % of baseline (BL), where the BL value of BAT SNA in each experiment is the minimum rms value of BAT SNA when the rat's  $T_{CORE}$  and  $T_{SKIN}$  are sufficiently warm ( $>37^{\circ}C$ ) to eliminate any cold-evoked BAT SNA. Pretreatment (ie, control) values of BAT SNA (expressed as % BL) and other variables were the mean values during the 60-s period before a treatment. Pretreatment control conditions varied depending on the experimental protocol. In some cases, we used a high  $T_{SKIN}$  and  $T_{CORE}$  ( $37.0^{\circ}C$ ), resulting in low levels of BAT SNA, or a low  $T_{SKIN}$  and  $T_{CORE}$  ( $35.0^{\circ}C$ ), which led to an elevated level (ie, cold-evoked) of pretreatment BAT SNA. In other cases, the pretreatment condition was during activation or inhibition of neuronal activity in brain regions (eg, DMH, rPa) within thermoregulatory circuits. The amplitudes of treatment-evoked responses were calculated from the mean levels of the variables during the 30 seconds period of the maximum response (either increase or decrease) occurring within 10 minutes of the treatment. The data are expressed as mean  $\pm$  SEM and compared with paired Student's *t*-test, with  $P < 0.05$  considered significant.

## ACKNOWLEDGEMENTS

We are grateful to Rubing Xing for histological assistance. We thank Dr. Kazuhiro Nakamura for a critical reading of an earlier version of this manuscript.

Funding information

NIH National Institute of Neurological Disorders and Stroke (NINDS), Grant/Award Number: NIH R01-NS091066

## REFERENCES

1. Nakamura K, Morrison SF. Preoptic mechanism for cold-defensive responses to skin cooling. *J Physiol*. 2008;586(10):2611–2620. [PubMed: 18388139]
2. Tanaka M, McKinley MJ, McAllen RM. Preoptic-raphe connections for thermoregulatory vasomotor control. *J Neurosci*. 2011;31(13):5078–5088. [PubMed: 21451045]
3. Nakamura K, Morrison SF. Central efferent pathways for cold-defensive and febrile shivering. *J Physiol*. 2011;589(Pt 14):3641–3658. [PubMed: 21610139]
4. Wanner SP, Almeida MC, Shimansky YP, et al. Cold-Induced Thermogenesis and Inflammation-Associated Cold-Seeking Behavior Are Represented by Different Dorsomedial Hypothalamic Sites: A Three-Dimensional Functional Topography Study in Conscious Rats. *J Neurosci*. 2017;37(29):6956–6971. [PubMed: 28630253]

5. Yahiro T, Kataoka N, Nakamura Y, Nakamura K. The lateral parabrachial nucleus, but not the thalamus, mediates thermosensory pathways for behavioural thermoregulation. *Sci Rep*. 2017;7(1): 5031. [PubMed: 28694517]
6. Nakamura Y, Nakamura K, Morrison SF. Different populations of prostaglandin EP3 receptor-expressing preoptic neurons project to two fever-mediating sympathoexcitatory brain regions. *Neuroscience*. 2009;161(2):614–620. [PubMed: 19327390]
7. Morrison SF. Central control of body temperature. *F1000Res*. 2016;5(880):1–10.
8. Morrison SF, Madden CJ. Central nervous system regulation of brown adipose tissue. *Compr Physiol*. 2014;4(4):1677–1713. [PubMed: 25428857]
9. Nakamura K. Central circuitries for body temperature regulation and fever. *Am J Physiol Regul Integr Comp Physiol*. 2011;301 (5):R1207–R1228. [PubMed: 21900642]
10. Nakamura K, Morrison SF. Central efferent pathways mediating skin cooling-evoked sympathetic thermogenesis in brown adipose tissue. *Am J Physiol Regul Integr Comp Physiol*. 2007;292(1): R127–R136. [PubMed: 16931649]
11. Tan CL, Cooke EK, Leib DE, et al. Warm-sensitive neurons that control body temperature. *Cell*. 2016;167(1):47–59. [PubMed: 27616062]
12. Bamshad M, Song CK, Bartness TJ. CNS origins of the sympathetic nervous system outflow to brown adipose tissue. *Am J Physiol*. 1999;276(6 Pt 2):R1569–R1578. [PubMed: 10362733]
13. Cano G, Passerin AM, Schiltz JC, Card JP, Morrison SF, Sved AF. Anatomical substrates for the central control of sympathetic outflow to interscapular adipose tissue during cold exposure. *J Comp Neurol*. 2003;460(3):303–326. [PubMed: 12692852]
14. Bratincsak A, Palkovits M. Activation of brain areas in rat following warm and cold ambient exposure. *Neuroscience*. 2004;127(2):385–397. [PubMed: 15262329]
15. Srividya R, Mallick HN, Kumar VM. Differences in the effects of medial and lateral preoptic lesions on thermoregulation and sleep in rats. *Neuroscience*. 2006;139(3):853–864. [PubMed: 16497443]
16. Zhao ZD, Yang WZ, Gao C, et al. A hypothalamic circuit that controls body temperature. *Proc Natl Acad Sci USA*. 2017;114 (8):2042–2047. [PubMed: 28053227]
17. Mount LE, Willmott JV. The relation between spontaneous activity, metabolic rate and the 24 hour cycle in mice at different environmental temperatures. *J Physiol*. 1967;190(2):371–380. [PubMed: 6049009]
18. Overton JM. Phenotyping small animals as models for the human metabolic syndrome: thermoneutrality matters. *Int J Obes*. 2010;34:S53.
19. Scimemi A, Beato M. Determining the neurotransmitter concentration profile at active synapses. *Mol Neurobiol*. 2009;40(3):289–306. [PubMed: 19844813]
20. Nakamura Y, Nakamura K, Matsumura K, Kobayashi S, Kaneko T, Morrison SF. Direct pyrogenic input from prostaglandin EP3 receptor-expressing preoptic neurons to the dorsomedial hypothalamus. *Eur J Neurosci*. 2005;22(12):3137–3146. [PubMed: 16367780]
21. Cao WH, Madden CJ, Morrison SF. Inhibition of brown adipose tissue thermogenesis by neurons in the ventrolateral medulla and in the nucleus tractus solitarius. *Am J Physiol Regul Integr Comp Physiol*. 2010;299(1):R277–R290. [PubMed: 20410479]
22. Morrison SF, Sved AF, Passerin AM. GABA-mediated inhibition of raphe pallidus neurons regulates sympathetic outflow to brown adipose tissue. *Am J Physiol*. 1999;276(2 Pt 2):R290–R297. [PubMed: 9950904]
23. Tupone D. An excitatory projection from median preoptic area to the dorsomedial hypothalamus contributes to the activation BAT thermogenesis. *FASEB J*. 2014;28(Suppl 1):1104.
24. Dimitrov EL, Kim YY, Usdin TB. Regulation of hypothalamic signaling by tuberoinfundibular peptide of 39 residues is critical for the response to cold: a novel peptidergic mechanism of thermoregulation. *J Neurosci*. 2011;31(49):18166–18179. [PubMed: 22159128]
25. Yu S, Qualls-Creekmore E, Rezai-Zadeh K, et al. Glutamatergic preoptic area neurons that express leptin receptors drive temperature-dependent body weight homeostasis. *J Neurosci*. 2016;36 (18): 5034–5046. [PubMed: 27147656]
26. Cao WH, Morrison SF. Disinhibition of rostral raphe pallidus neurons increases cardiac sympathetic nerve activity and heart rate. *Brain Res*. 2003;980(1):1–10. [PubMed: 12865154]

27. Cao WH, Morrison SF. Glutamate receptors in the raphe pallidus mediate brown adipose tissue thermogenesis evoked by activation of dorsomedial hypothalamic neurons. *Neuropharmacology*. 2006;51(3):426–437. [PubMed: 16733059]
28. Nakamura K, Matsumura K, Kaneko T, Kobayashi S, Katoh H, Negishi M. The rostral raphe pallidus nucleus mediates pyrogenic transmission from the preoptic area. *J Neurosci*. 2002;22 (11): 4600–4610. [PubMed: 12040067]
29. Yoshida K, Li X, Cano G, Lazarus M, Saper CB. Parallel preoptic pathways for thermoregulation. *J Neurosci*. 2009;29 (38):11954–11964. [PubMed: 19776281]
30. Madden CJ, Morrison SF. Excitatory amino acid receptor activation in the raphe pallidus area mediates prostaglandin-evoked thermogenesis. *Neuroscience*. 2003;122(1):5–15. [PubMed: 14596844]
31. Cao WH, Fan W, Morrison SF. Medullary pathways mediating specific sympathetic responses to activation of dorsomedial hypothalamus. *Neuroscience*. 2004;126(1):229–240. [PubMed: 15145088]
32. Tanaka M, Owens NC, Nagashima K, Kanosue K, McAllen RM. Reflex activation of rat fusimotor neurons by body surface cooling, and its dependence on the medullary raphe. *J Physiol*. 2006;572(Pt 2):569–583. [PubMed: 16484305]
33. Zhang YH, Yanase-Fujiwara M, Hosono T, Kanosue K. Warm and cold signals from the preoptic area: which contribute more to the control of shivering in rats? *J Physiol*. 1995;485(Pt 1):195–202. [PubMed: 7658373]
34. Kataoka N, Hioki H, Kaneko T, Nakamura K. Psychological stress activates a dorsomedial hypothalamus-medullary raphe circuit driving brown adipose tissue thermogenesis and hyperthermia. *Cell Metab*. 2014;20(2):346–358. [PubMed: 24981837]
35. Machado N, Abbott S, Resch JM, et al. A glutamatergic hypothalamomedullary circuit mediates thermogenesis, but not heat conservation, during stress-induced hyperthermia. *Curr Biol*. 2018;28 (14):2291–2301. [PubMed: 30017482]
36. Chen XM, Hosono T, Yoda T, Fukuda Y, Kanosue K. Efferent projection from the preoptic area for the control of non-shivering thermogenesis in rats. *J Physiol*. 1998;512(Pt 3):883–892. [PubMed: 9769429]
37. Rothwell NJ, Stock MJ, Thexton AJ. Decerebration activates thermogenesis in the rat. *J Physiol (Lond)*. 1983;342:15–22. [PubMed: 6631729]
38. Tupone D, Cano G, Morrison SF. Thermoregulatory inversion: a novel thermoregulatory paradigm. *Am J Physiol Regul Integr Comp Physiol*. 2017;312(5):R779–R786. [PubMed: 28330964]
39. Shibata M, Iriki M, Arita J, et al. Procaine microinjection into the lower midbrain increases brown fat and body temperatures in anesthetized rats. *Brain Res*. 1996;716(1-2):171–179. [PubMed: 8738234]
40. Uschakov A, Gong H, McGinty D, Szymusiak R. Efferent projections from the median preoptic nucleus to sleep- and arousal-regulatory nuclei in the rat brain. *Neuroscience*. 2007;150 (1):104–120. [PubMed: 17928156]
41. Nakamura K, Morrison SF. A thermosensory pathway mediating heat-defense responses. *Proc Natl Acad Sci USA*. 2010;107 (19):8848–8853. [PubMed: 20421477]
42. Abbott S, Saper CB. Median preoptic glutamatergic neurons promote thermoregulatory heat loss and water consumption in mice. *J Physiol*. 2017;595(20):6569–6583. [PubMed: 28786483]
43. Chou TC, Bjorkum AA, Gaus SE, Lu J, Scammell TE, Saper CB. Afferents to the ventrolateral preoptic nucleus. *J Neurosci*. 2002;22(3):977–990. [PubMed: 11826126]
44. Mohammed M, Madden CJ, Morrison SF. Ventral lateral preoptic (vLPO) neurons inhibit brown adipose tissue thermogenesis during warming of the preoptic area. *FASEB J*. 2018;1 Available at: [https://www.fasebj.org/doi/10.1096/fasebj.2018.32.1\\_supplement.592.7](https://www.fasebj.org/doi/10.1096/fasebj.2018.32.1_supplement.592.7). Accessed 1\_supplement: 592.7, 32.
45. Kashio M, Tominaga M. The TRPM2 channel: a thermo-sensitive metabolic sensor. *Channels*. 2017;11(5):426–433. [PubMed: 28633002]
46. Song K, Wang H, Kamm GB, et al. The TRPM2 channel is a hypothalamic heat sensor that limits fever and can drive hypothermia. *Science*. 2016;353(6306):1393–1398. [PubMed: 27562954]



47. Duarte JO, Gomes KS, Nunes-de-Souza RL, Crestani CC. Role of the lateral preoptic area in cardiovascular and neuroendocrine responses to acute restraint stress in rats. *Physiol Behav.* 2017;175:16–21. [PubMed: 28342768]
48. Osaka T Cold-induced thermogenesis mediated by GABA in the preoptic area of anesthetized rats. *Am J Physiol Regul Integr Comp Physiol.* 2004;287(2):R306–R313. [PubMed: 15031132]
49. Sherin JE, Shiromani PJ, McCarley RW, Saper CB. Activation of ventrolateral preoptic neurons during sleep. *Science.* 1996;271 (5246):216–219. [PubMed: 8539624]
50. Saito YC, Maejima T, Nishitani M, et al. Monoamines inhibit GABAergic neurons in ventrolateral preoptic area that make direct synaptic connections to hypothalamic arousal neurons. *J Neurosci.* 2018;38(28):6366–6378. [PubMed: 29915137]
51. Madden CJ, Tupone D, Cano G, Morrison SF. Alpha2 Adrenergic receptor-mediated inhibition of thermogenesis. *J Neurosci.* 2013;33(5):2017–2028. [PubMed: 23365239]
52. Conceicao EP, Madden CJ, Morrison SF. Glycinergic inhibition of BAT sympathetic premotor neurons in rostral raphe pallidus. *Am J Physiol Regul Integr Comp Physiol.* 2017;312(6):R919–R926. [PubMed: 28254751]
53. Giuliano R, Ruggiero DA, Morrison S, Ernsberger P, Reis DJ. Cholinergic regulation of arterial pressure by the C1 area of the rostral ventrolateral medulla. *J Neurosci.* 1989;9:923–942. [PubMed: 2926485]
54. Paxinos G, Watson C. *The Rat Brain in Stereotaxic Coordinates.* 6th ed. San Diego: Academic Press: Elsevier; 2007.

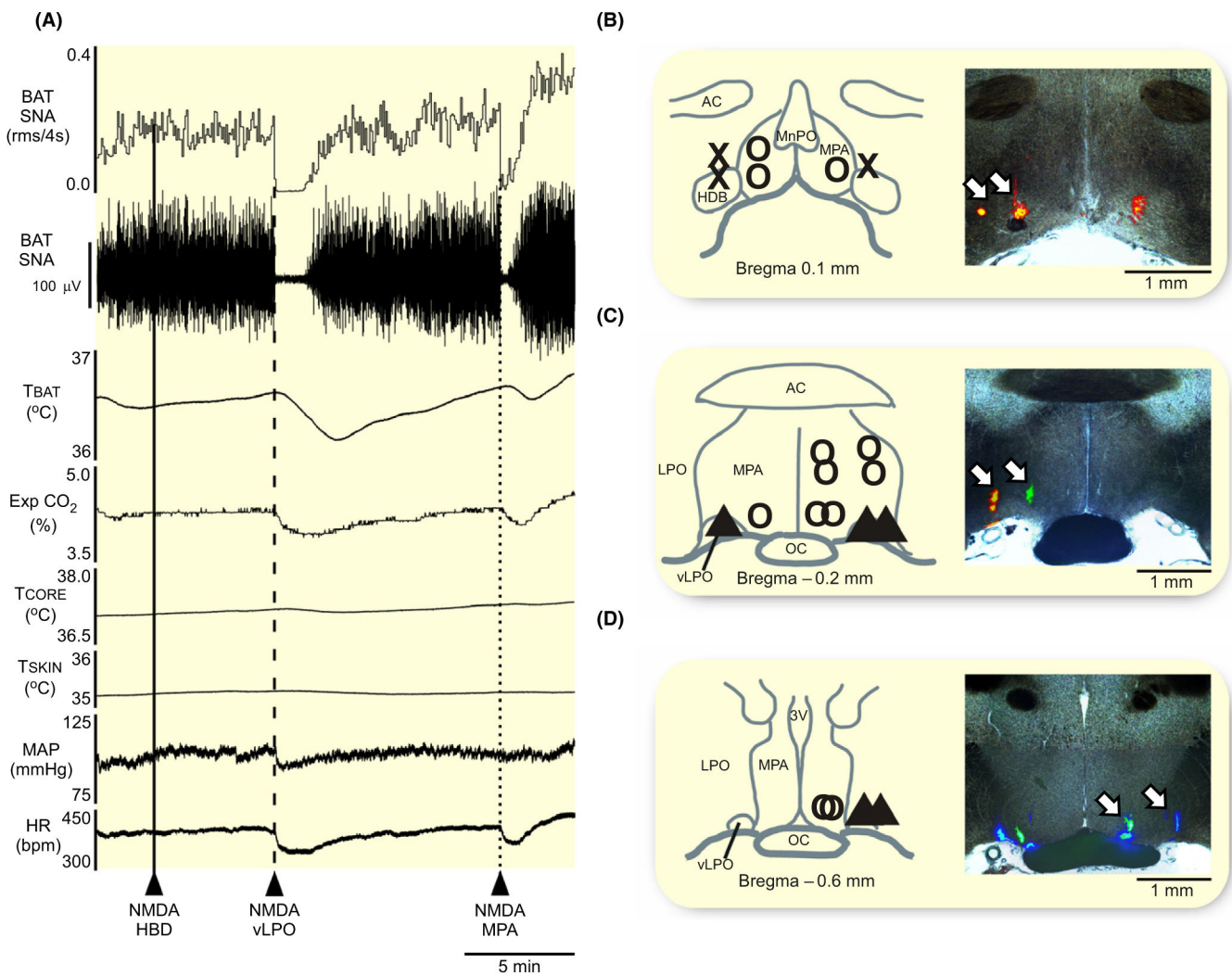


**FIGURE 1.**

Injection of NMDA into vLPO or into MPA inhibits the BAT thermogenesis evoked by cold exposure. A, Nanoinjections of N-methyl-D-aspartate (NMDA, 0.2 mmol/L, 60 nL) in the region of the horizontal limb of the diagonal band of Broca (HDB, solid line) had no effect on brown adipose tissue sympathetic nerve activity (BAT SNA), BAT temperature ( $T_{BAT}$ ), expired  $CO_2$  (Exp  $CO_2$ ), core body temperature ( $T_{CORE}$ ), mean arterial pressure (MAP) or heart rate (HR). In contrast, nanoinjections of NMDA into the ventral part of the lateral preoptic area (vLPO, dashed line) or into the medial preoptic area (MPA; dotted line) significantly inhibited BAT SNA and reduced  $T_{BAT}$ , Exp  $CO_2$ , and HR. B–D, Composite maps of the NMDA nanoinjection sites plotted on schematic drawings through the preoptic area (POA) at +0.1 mm (B), –0.2 mm (C), and –0.6 mm (D) from bregma, accompanied by corresponding histological sections containing the fluorescent beads marking representative NMDA nanoinjection sites (white arrows). X: indicates injections targeting the region of the HDB, ▲: indicates injections targeting the vLPO, and O: indicates injections targeting the MPA. 3 V, third ventricle; ac, anterior commissure; LPO, lateral preoptic; MnPO, median preoptic area; oc, optic chiasm;

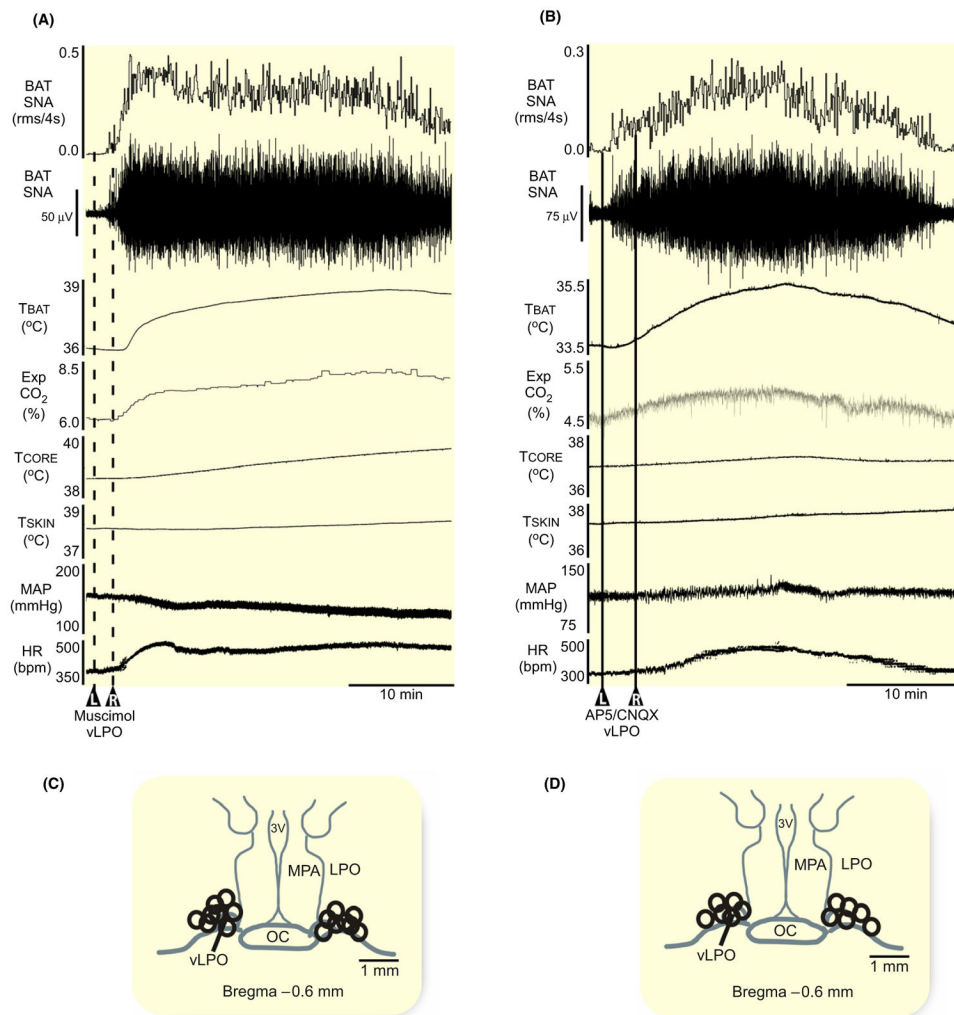


**FIGURE 2.** Activation of GABA<sub>A</sub> receptors or blockade of glutamate receptors in the vLPO increases BAT thermogenesis. A, Bilateral nano-injections of muscimol (1.2 mmol/L, 60 nL, dashed line, n = 8) in the vLPO increased BAT SNA, BAT temperature (T<sub>BAT</sub>), expired CO<sub>2</sub> (Exp CO<sub>2</sub>), core temperature (T<sub>CORE</sub>), mean arterial pressure (MAP), and heart rate (HR). B, Bilateral nano-injections of AP5/CNQX (5 mmol/L each, 60 nL, solid line, n = 4) in the vLPO increased BAT SNA, T<sub>BAT</sub>, Exp CO<sub>2</sub>, T<sub>CORE</sub>, MAP, and HR. C and D, Composite mapping of the muscimol and AP5/CNQX nano-injection sites plotted on drawing of vLPO at -0.6 mm caudal to bregma. 3 V, third ventricle; oc, optic chiasm; LPO, lateral preoptic; MPA, medial preoptic area; vLPO, ventral part of the lateral preoptic area

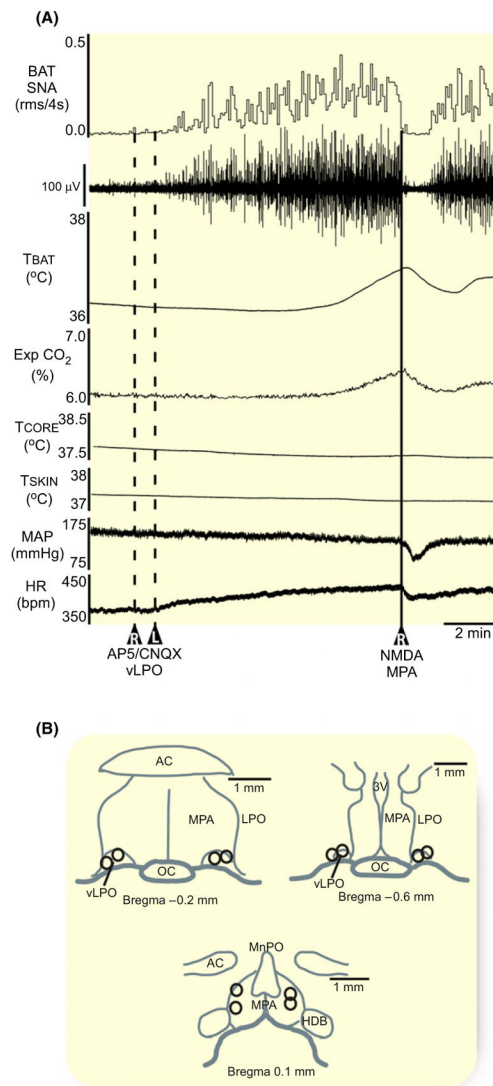


**FIGURE 3.**

Nanoinjection of NMDA in the MPA inhibits BAT thermogenesis evoked by blockade of glutamate receptors in the vLPO. A, A unilateral nanoinjection of NMDA (0.2 mmol/L, 60 nL, solid line) in the medial preoptic area (MPA) reversed the increases in BAT SNA, BAT temperature ( $T_{BAT}$ ), expired  $CO_2$  (Exp  $CO_2$ ), and heart rate (HR) elicited by bilateral nanoinjections of AP5/CNQX (5 mmol/L each, 60 nL, dashed lines) in the vLPO. B, composite map of the AP5/CNQX nanoinjection sites ( $n = 4$  pairs) plotted on drawings through the vLPO at  $-0.2$  mm and  $-0.6$  mm caudal to bregma; composite map of the NMDA nanoinjection sites ( $n = 4$ ) plotted on a drawing through the MPA at  $+0.2$  mm rostral to bregma. ac, anterior commissure;  $T_{CORE}$ , core temperature; HDB, diagonal band of Broca; LPO, lateral preoptic; MAP, mean arterial pressure; MPA, medial preoptic area; MnPO, median preoptic area; oc, optic chiasm; 3 V, third ventricle; vLPO, ventral part of the lateral preoptic area

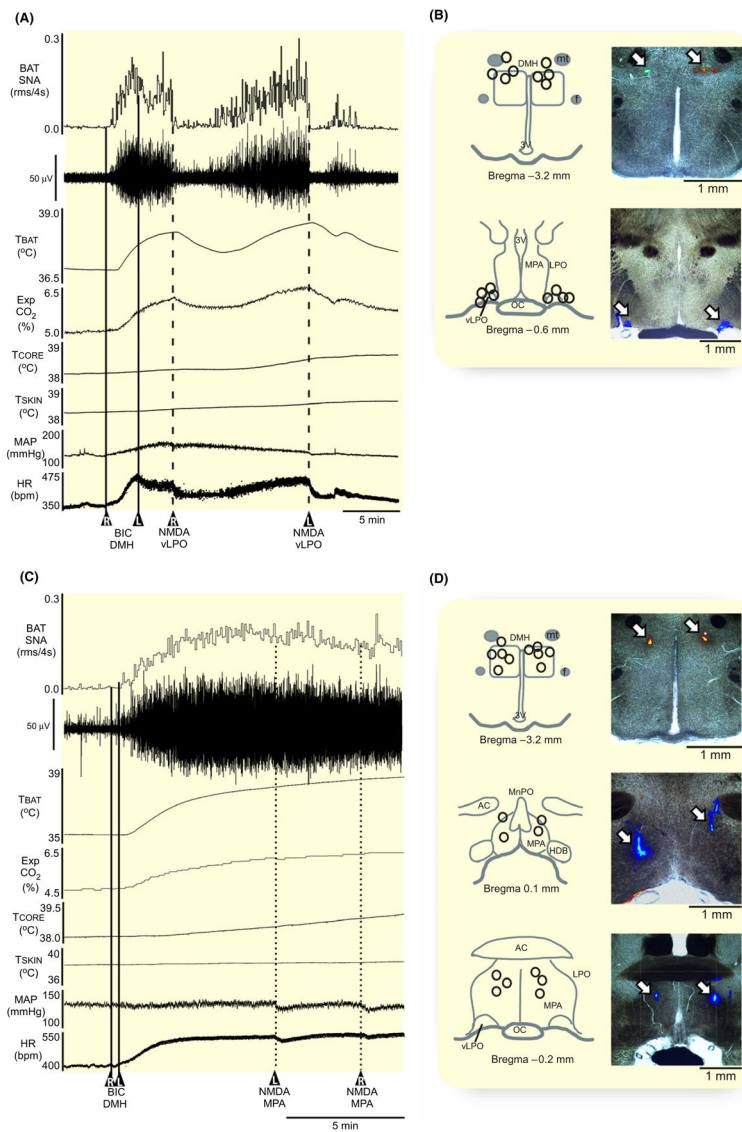


**FIGURE 4.** Hypothermic action of MPA, but not of vLPO, requires GABAergic input to DMH. A, Nanoinjections of NMDA (0.2 mmol/L, 60 nL) in the vLPO inhibited the elevated levels of BAT SNA, BAT temperature ( $T_{BAT}$ ), expired  $CO_2$  ( $Exp\ CO_2$ ), core temperature ( $T_{CORE}$ ), mean arterial pressure (MAP), and heart rate (HR) evoked by bilateral nanoinjection of bicuculline (BIC, 1 mmol/L, 60 nL; straight line;  $n = 4$ ) in the dorsomedial hypothalamus (DMH). B, composite mapping of the BIC nanoinjection sites plotted on drawing of DMH at  $-3.2$  mm caudal to bregma; composite mapping of the NMDA nanoinjection sites plotted on drawing of vLPO at  $-0.6$  mm caudal to bregma; and histological section containing the fluorescent beads marking a representative nanoinjection. C, Nanoinjections of NMDA (0.2 mmol/L, 60 nL) in the medial preoptic area (MPA) do not affect the elevated levels of BAT SNA,  $T_{BAT}$ ,  $Exp\ CO_2$ ,  $T_{CORE}$ , MAP, and HR evoked by bilateral nanoinjection of BIC (1 mmol/L, 60 nL; straight line;  $n = 5$ ) in the dorsomedial hypothalamus (DMH). D, composite mapping of the BIC nanoinjection sites plotted on drawing of DMH at  $-3.2$  mm caudal to

bregma; composite mapping of the NMDA nanoinjection sites plotted on drawing of MPA at 0.1 mm and -0.2 mm from bregma; and histological section containing the fluorescent beads marking a representative nanoinjection. ac, anterior commissure; DMH, dorsomedial hypothalamus; HDB, diagonal band of Broca; f, fornix; LPO, lateral preoptic; MPA, medial preoptic area; MnPO, median preoptic area; oc, optic chiasm; mt, mammillothalamic tract; 3 V, third ventricle; vLPO, ventral part of the lateral preoptic area

Author Manuscript

Author Manuscript

Author Manuscript

Author Manuscript

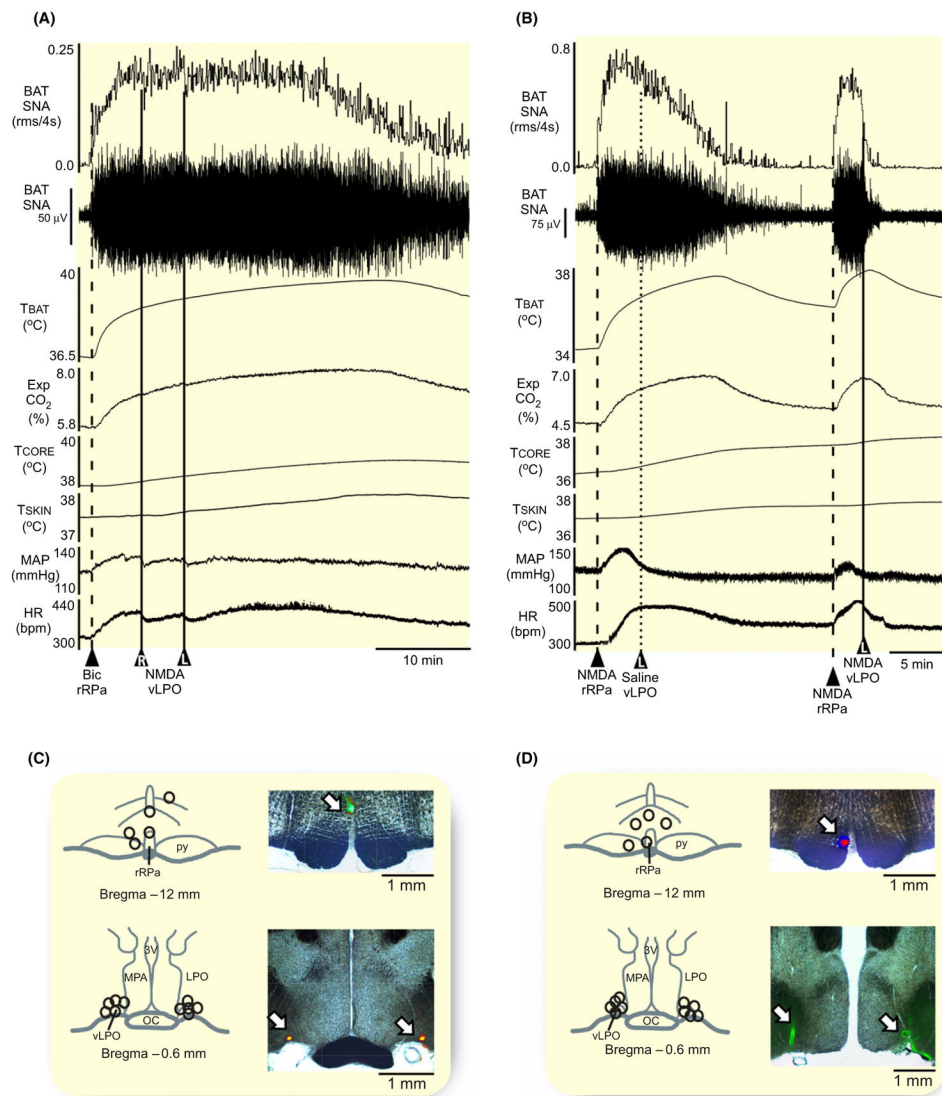


**FIGURE 5.**

Activation of vLPO neurons inhibits BAT thermogenesis evoked by nanoinjection of NMDA, but not bicuculline, in rRPa. A, Nanoinjections of NMDA (0.2 mmol/L, 60 nL) in the vLPO revert the elevated levels of BAT SNA, BAT temperature ( $T_{BAT}$ ), expired  $CO_2$  (Exp  $CO_2$ ), core temperature ( $T_{CORE}$ ), mean arterial pressure (MAP), and heart rate (HR) evoked by bicuculline (1 mmol/L, 60 nL) nanoinjection in the rRPa. B, Nanoinjections of NMDA (0.2 mmol/L, 60 nL) in the vLPO on the elevated levels of BAT SNA,  $T_{BAT}$ , Exp  $CO_2$ ,  $T_{CORE}$ , MAP, and HR evoked by nanoinjection of NMDA (0.2 mmol/L, 60 nL) in the rRPa. C, composite mapping of the NMDA nanoinjection sites plotted on drawing of rRPa at -12 mm caudal to bregma; composite mapping of the NMDA nanoinjection sites plotted on drawing of vLPO at -0.6 mm caudal to bregma; and histological section containing the fluorescent beads marking a representative nanoinjection. D, Composite mapping of the bicuculline nanoinjection sites plotted on drawing of rRPa at -12 mm caudal to bregma; and composite mapping of the NMDA nanoinjection sites plotted on drawing of vLPO at -0.6 mm caudal to bregma; and histological section containing the fluorescent beads marking a

representative nanoinjection. LPO, lateral preoptic; MPA, medial preoptic area; oc, optic chiasm; py, pyramidal tract; rRPa, rostral raphe pallidus; 3 V, third ventricle; vLPO, ventral part of the lateral preoptic area.

Author Manuscript

Author Manuscript

Author Manuscript

Author Manuscript



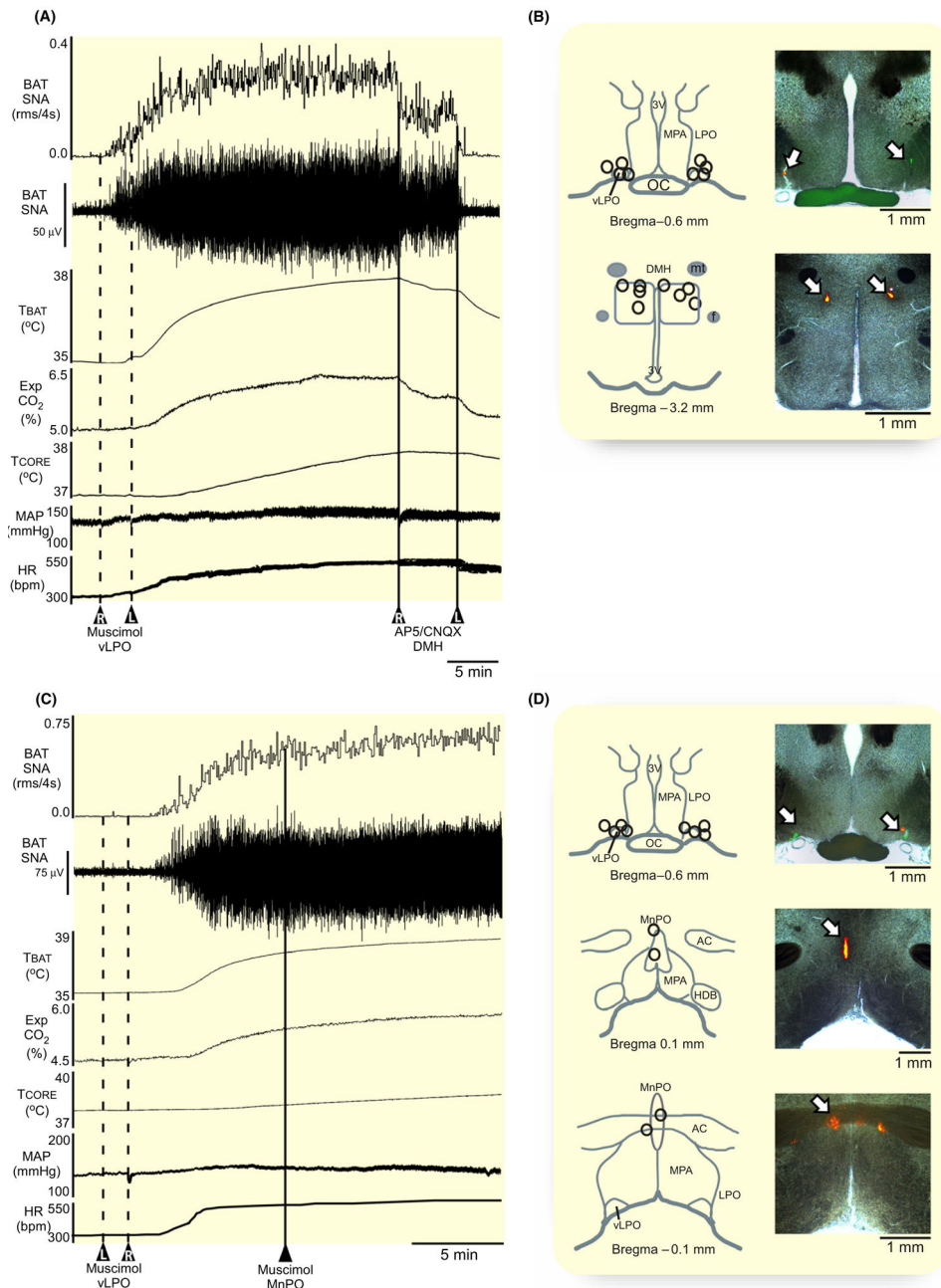


**FIGURE 6.** Effect of blockade of ionotropic glutamate receptors in DMH or inhibition of MnPO neurons on the BAT thermogenesis evoked by inhibition of vLPO neurons. A, bilateral nanoinjection of AP5/CNQX (straight line; 60 nL; AP5 and CNQX, 5 mmol/L each; n = 4) in the dorsomedial hypothalamus (DMH) terminate the raise of BAT SNA, BAT temperature (T<sub>BAT</sub>), expired CO<sub>2</sub> (Exp CO<sub>2</sub>), core temperature (T<sub>core</sub>), mean arterial pressure (MAP), and heart rate (HR) evoked by bilateral nanoinjections of muscimol (1.2 mmol/L, 60 nL) in vLPO. B, composite mapping of the muscimol nanoinjection sites plotted on drawing of vLPO at -0.6 mm caudal to bregma; composite mapping of the AP5/CNQX nanoinjection sites plotted on drawing of DMH at -3.2 mm caudal to bregma; and histological section

containing the fluorescent beads marking a representative nano-injection. D, nano-injection of muscimol (1.2 mmol/L, 60 nL; straight line; n = 4) in the median preoptic area (MnPO) does not affect the raise of BAT SNA,  $T_{BAT}$ ,  $T_{CORE}$ , Exp  $CO_2$ , MAP, and HR evoked by bilateral nano-injections of muscimol (1.2 mmol/L, 60 nL; dashed line; n = 4) in vLPO. E, composite mapping of the muscimol nano-injection sites plotted on drawing of vLPO at -0.6 mm caudal to bregma; composite mapping of the muscimol nano-injection sites plotted on drawing of MnPO at 0.1 mm and -0.1 mm from bregma; and histological section containing the fluorescent beads marking a representative nano-injection. ac, anterior commissure; DMH, dorsomedial hypothalamus; f, fornix; HDB, diagonal band of Broca; LPO, lateral preoptic; MnPO, median preoptic area; MPA, medial preoptic area; mt, mammillothalamic tract; oc, optic chiasm; 3 V, third ventricle; vLPO, ventral part of the lateral preoptic area

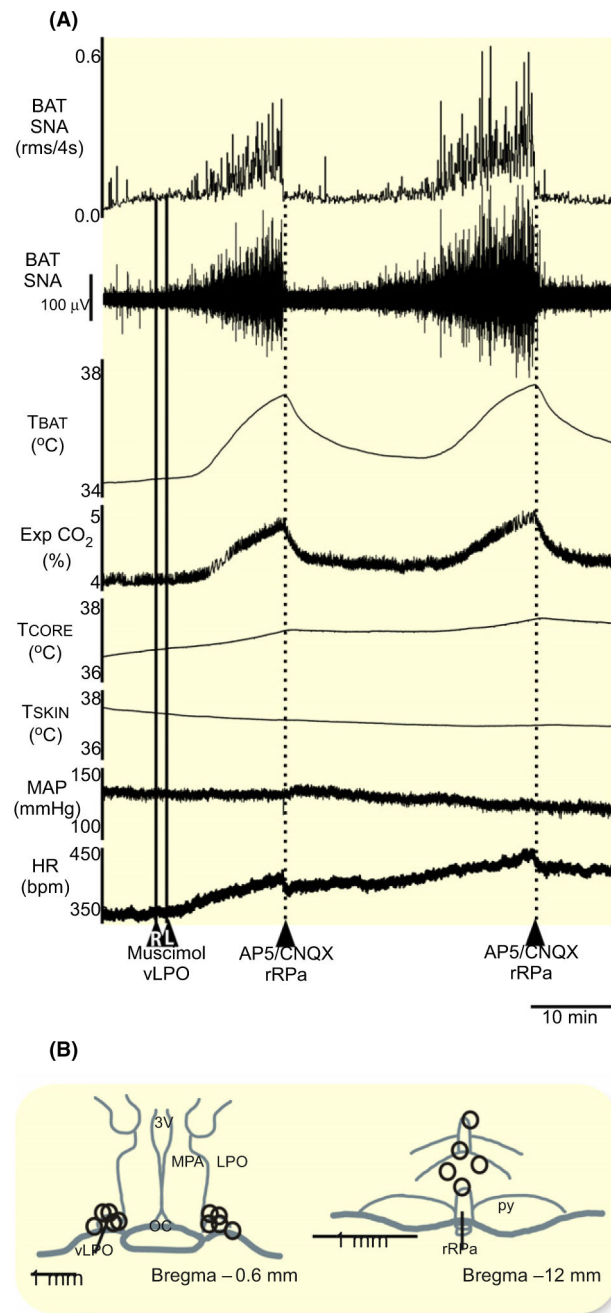


**FIGURE 7.** Nanoinjections of AP5/CNQX in the rRPa inhibit BAT thermogenesis elicited by vLPO inhibition. A, Nanoinjection of AP5/CNQX (dashed line; 60 nL; AP5 and CNQX, 5 mmol/L each; n = 4) into rostral raphe pallidus (rRPa) inhibited the increases in BAT SNA, BAT temperature ( $T_{BAT}$ ), expired  $CO_2$  ( $Exp\ CO_2$ ), core temperature ( $T_{CORE}$ ), mean arterial pressure (MAP), and heart rate (HR) evoked by vLPO inhibition with bilateral nanoinjections muscimol (1.2 mmol/L, 60 nL, straight line, n = 4). B, composite mapping of the muscimol nanoinjection sites plotted on drawing of vLPO at -0.6 mm caudal to bregma. C, composite mapping of the AP5/CNQX nanoinjection sites plotted on drawing of rRPa at

–12 mm caudal to bregma. ac, anterior commissure; LPO, lateral preoptic; MPA, medial preoptic area; oc, optic chiasm; py, pyramidal tract; rRPa, rostral raphe pallidus; 3 V, third ventricle; vLPO, ventral part of the lateral preoptic area

Author Manuscript

Author Manuscript

Author Manuscript

Author Manuscript

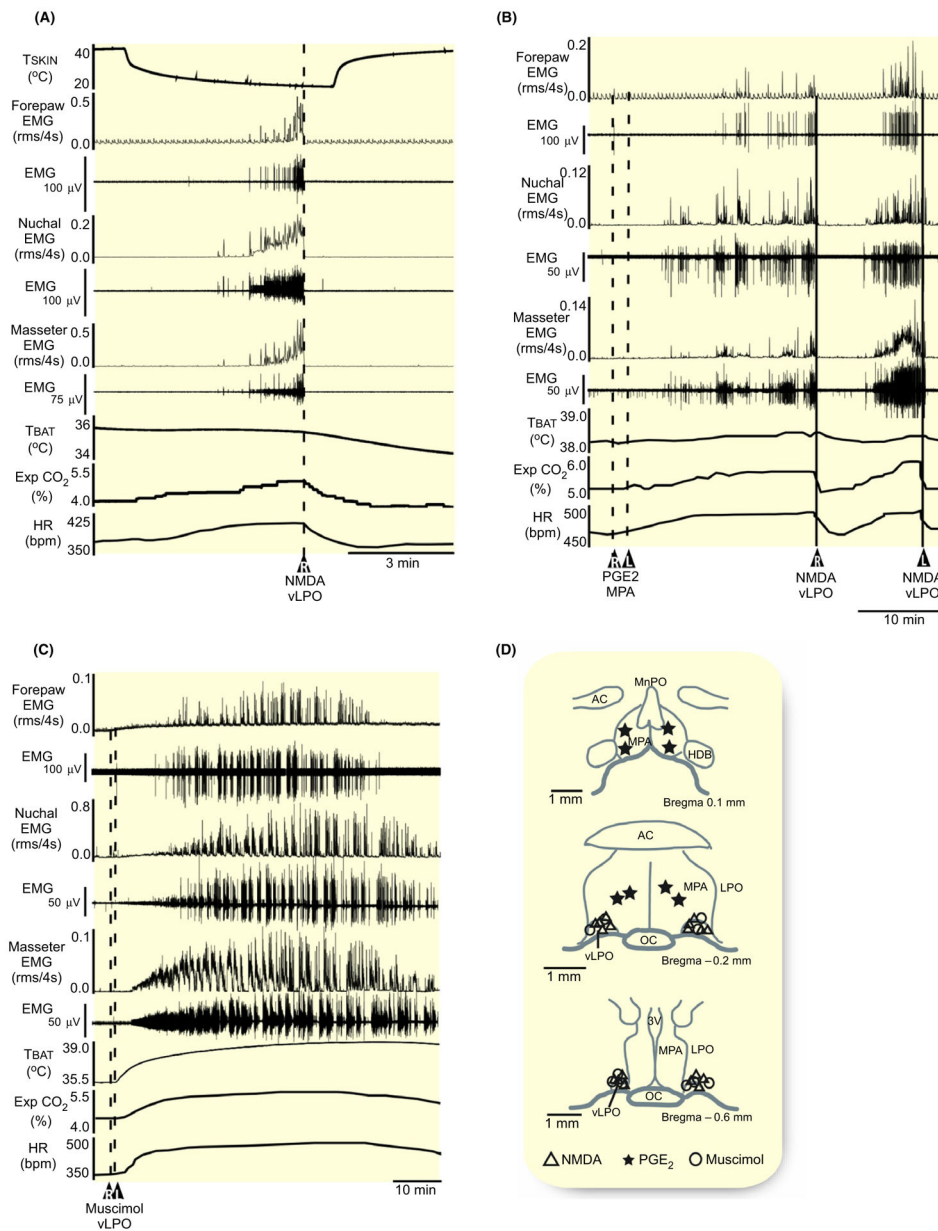


**FIGURE 8.**

NMDA nanoinjections in the vLPO inhibit skin cooling and prostaglandin-evoked muscle shivering. A, Effect of nanoinjections of NMDA (0.2 mmol/L, 60 nL, dashed line, n = 6) in the vLPO on the muscle shivering EMG amplitudes in masseter, nuchal, and forelimb muscles, and on BAT temperature ( $T_{BAT}$ ), expired  $CO_2$  (Exp  $CO_2$ ), and heart rate (HR) during rapid skin cooling. B, Effect of nanoinjections of NMDA (0.2 mmol/L, 60 nL, straight line, n = 4) in the vLPO on the muscle shivering EMG amplitudes in masseter, nuchal, and forelimb muscles, and on  $T_{BAT}$ , Exp  $CO_2$ , and HR responses evoked by nanoinjections of PGE<sub>2</sub> injections (1 mg/mL, 60 nL, dashed line, n = 4) in the MPA. C, Effect of bilateral nanoinjections of muscimol (1.2 mmol/L, 60 nL, dashed line, n = 4) in the vLPO on the muscle shivering EMG amplitudes in masseter, nuchal, and forelimb muscles,

and on T<sub>BAT</sub>, Exp CO<sub>2</sub>, and HR. D, composite mapping of the PGE<sub>2</sub> nano-injection sites plotted on drawing of MPA at 0.1 mm and -0.2 mm from bregma and of the NMDA and muscimol nano-injection sites plotted on drawing of vLPO at -0.2 mm and -0.6 mm caudal to bregma. ac, anterior commissure; HDB, diagonal band of Broca; LPO, lateral preoptic; MnPO, medial preoptic area; MPA, medial preoptic area; oc, optic chiasm; 3 V, third ventricle; vLPO, ventral part of the lateral preoptic area

Author Manuscript

Author Manuscript

Author Manuscript

Author Manuscript

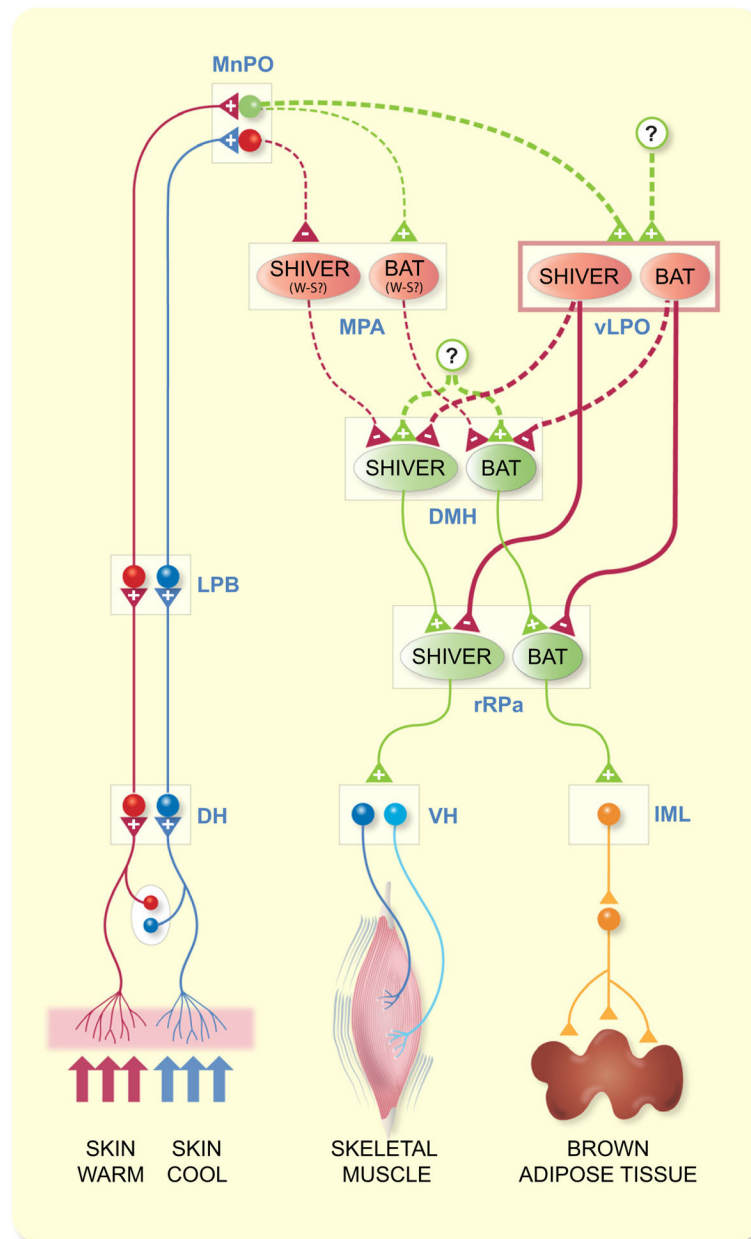


**FIGURE 9.** An extension of the proposed<sup>7</sup> schematic model of the thermoregulatory reflex circuit for the regulation of BAT and shivering thermogenesis by cutaneous thermoreceptors: proposed role for neurons in the vLPO. Cool and warm cutaneous thermoreceptors transmit signals to respective primary sensory neurons in the dorsal root ganglia (DRG) which relay this information to the second-order thermal sensory neurons in the dorsal horn (DH). Cool-activated and warm-activated DH neurons excite the third-order sensory neurons in the external lateral subnucleus of the lateral parabrachial nucleus (LPB) and in the dorsal subnucleus of the LPB respectively. Neurons in the median preoptic (MnPO) subnucleus of the preoptic area (POA) receive these thermosensory signals from the LPB. Distinct populations (BAT: red circles; shivering: red ovals) of GABAergic, potentially warm-

sensitive (W-S), neurons in the medial preoptic area (MPA) are postulated (dashed lines) to inhibit (red lines) separate populations of BAT and shivering thermogenesis-promoting neurons in the dorsomedial hypothalamus (DMH). Cooling-activated, GABAergic MnPO interneurons are postulated (dashed lines) to inhibit MPA GABAergic neurons during cold exposure, thereby disinhibiting thermogenesis-promoting neurons in the DMH. DMH neurons also receive a tonic excitation from an unknown (?) source. Distinct populations (BAT: red circles; shivering: red ovals) of GABAergic neurons in the ventral part of the lateral preoptic area (vLPO) inhibit respectively, sympathetic and shivering premotor neurons in the rostral raphe pallidus (rRPa). vLPO neurons may (dashed lines) inhibit thermogenesis-promoting neurons in the DMH. Warm-activated MnPO neurons are postulated (dashed lines) to excite (green lines) MPA GABAergic neurons, leading to warm-activated inhibition of thermogenesis-promoting neurons in the DMH. MnPO glutamatergic neurons may (dashed lines) provide a warm-activated excitatory drive to vLPO GABAergic neurons. Thermogenesis-inhibiting neurons in the vLPO may receive an excitatory input (green dashed lines) from an unknown (?) source. Sympathetic preganglionic neurons (SPNs) in the intermediolateral nucleus (IML) and alpha ( $\alpha$ ) and gamma ( $\gamma$ ) motoneurons in the ventral horn (VH) of the spinal cord are excited by their antecedent premotor neuron populations in the rRPa to drive BAT and shivering thermogenesis respectively



**TABLE 1**

Effect of injecting NMDA into sites in the POA on the cooling-evoked activation of BAT and cardiovascular variables

	NMDA in HDB	NMDA in vLPO	NMDA in MPA
BAT SNA (%BL)	-171 ± 224 ( <i>P</i> = 0.1) pre-NMDA: 2202 ± 1729	-1929 ± 1838 ( <i>P</i> = 0.04) pre-NMDA: 2066 ± 1884	-1678 ± 1303 ( <i>P</i> = 0.001) pre-NMDA: 1881 ± 1471
T <sub>BAT</sub> (°C)	+0.1 ± 0.1 ( <i>P</i> = 0.02) pre-NMDA: 35.9 ± 1.0	-0.4 ± 0.1 ( <i>P</i> = 0.0004) pre-NMDA: 36.7 ± 0.7	-0.3 ± 0.2 ( <i>P</i> = 0.001) pre-NMDA: 36.4 ± 0.9
Exp CO <sub>2</sub> (%)	+0.1 ± 0.1 ( <i>P</i> = 0.04) pre-NMDA: 5.0 ± 0.8	-0.4 ± 0.1 ( <i>P</i> = 0.001) pre-NMDA: 5.0 ± 0.5	-0.3 ± 0.2 ( <i>P</i> = 0.0003) pre-NMDA: 5.1 ± 0.6
MAP (mmHg)	+5 ± 10 ( <i>P</i> = 0.2) pre-NMDA: 112 ± 24	-13 ± 10 ( <i>P</i> = 0.02) pre-NMDA: 129 ± 14	-10 ± 9 ( <i>P</i> = 0.005) pre-NMDA: 120 ± 16
HR (bpm)	-1 ± 16 ( <i>P</i> = 0.5) pre-NMDA: 404 ± 32	-46 ± 8 ( <i>P</i> = 0.0001) pre-NMDA: 427 ± 17	-43 ± 20 ( <i>P</i> = 0.0001) pre-NMDA: 422 ± 23

Changes in brown adipose tissue (BAT) sympathetic nerve activity (SNA), BAT temperature (TBAT), expired CO<sub>2</sub> (Exp CO<sub>2</sub>), mean arterial pressure (MAP), and heart rate (HR) following nano-injections of NMDA (0.2 mmol/L, 60 nL) into the region of the horizontal limb of the diagonal band of Broca (HDB), into the ventral lateral preoptic area (vLPO), and into the medial preoptic area (MPA). NMDA was injected (Figure 1A, n = 20) during an episode of skin cooling which elevated BAT SNA and BAT thermogenesis, and pre-NMDA values are those skin cooling-evoked levels during the 30 seconds period prior to the nano-injection of NMDA. *P* values compare the values of physiologic parameters between before and after the nano-injection of NMDA.

TABLE 2

Effect of inhibiting neurons in the vLPO on physiological variables

	Muscimol in the vLPO	AP5/CNQX in the vLPO
BAT SNA(%BL)	+2176 ± 1471 ( <i>P</i> = 0.002) pre-muscimol: 172 ± 90	+945 ± 721 ( <i>P</i> = 0.3) pre-AP5/CNQX: 115 ± 7
T <sub>BAT</sub> (°C)	+2.2 ± 0.8 ( <i>P</i> = 0.0001) pre-muscimol: 36.0 ± 1.2	+2.4 ± 0.8 ( <i>P</i> = 0.0001) pre-AP5/CNQX: 34.0 ± 0.8
Exp CO <sub>2</sub> (%)	+1.0 ± 0.3 ( <i>P</i> = 0.00003) pre-muscimol: 5.6 ± 1.2	+0.9 ± 0.6 ( <i>P</i> = 0.00003) pre-AP5/CNQX: 5.6 ± 0.7
T <sub>CORE</sub> (°C)	+0.7 ± 0.8 ( <i>P</i> = 0.02) pre-muscimol: 37.9 ± 1.0	+0.4 ± 0.4 ( <i>P</i> = 0.2) pre-AP5/CNQX: 37.0 ± 0.2
MAP(mmHg)	+5 ± 6 ( <i>P</i> = 0.02) pre-muscimol: 119 ± 21	-6 ± 14 ( <i>P</i> = 0.2) pre-AP5/CNQX: 125 ± 12
HR (bpm)	+67 ± 52 ( <i>P</i> = 0.01) pre-muscimol: 359 ± 29	+42 ± 43 ( <i>P</i> = 0.1) pre-AP5/CNQX: 383 ± 48

Changes in brown adipose tissue (BAT) sympathetic nerve activity (SNA), BAT temperature (T<sub>BAT</sub>), expired CO<sub>2</sub> (Exp CO<sub>2</sub>), mean arterial pressure (MAP), and heart rate (HR) following nano-injections of muscimol (1.2 mmol/L, 60 nL, n = 8) and AP5/CNQX (5 mmol/L each, 60 nL, n = 6) in the ventral lateral preoptic area (vLPO). Muscimol and AP5/CNQX were injected under thermoneutral condition (Figure 2A,C respectively) in the absence of BAT SNA.

*P* values refer to the differences between the pre-muscimol and pre-AP5/CNQX values of the physiologic parameters and the peak values after the nano-injections in the vLPO.

**TABLE 3**

Effect of activating MPA and vLPO neurons during the BAT sympathoexcitation evoked by disinhibition of DMH

	<b>NMDA in the vLPO after BIC in DMH</b>	<b>NMDA in the MPA after BIC in DMH</b>
BAT SNA (%BL)	$-758 \pm 545$ ( $P=0.03$ ) pre-NMDA: $921 \pm 657$	$+15 \pm 148$ ( $P=0.4$ ) pre-NMDA: $1867 \pm 1228$
T <sub>BAT</sub> (°C)	$-0.6 \pm 0.2$ ( $P=0.01$ ) pre-NMDA: $37.9 \pm 0.7$	$+0.2 \pm 0.1$ ( $P=0.001$ ) pre-NMDA: $37.8 \pm 0.7$
Exp CO <sub>2</sub> (%)	$-0.3 \pm 0.1$ ( $P=0.004$ ) pre-NMDA: $6.5 \pm 1.4$	$+0.1 \pm 0.0$ ( $P=0.001$ ) pre-NMDA: $5.8 \pm 0.4$
T <sub>CORE</sub> (°C)	$-0.2 \pm 0.6$ ( $P=0.2$ ) pre-NMDA: $38.5 \pm 0.5$	$+0.1 \pm 0.0$ ( $P=0.1$ ) pre-NMDA: $38.0 \pm 0.8$
MAP(mmHg)	$-7 \pm 6$ ( $P=0.04$ ) pre-NMDA: $143 \pm 14$	$+1 \pm 4$ ( $P=0.3$ ) pre-NMDA: $135 \pm 4$
HR (bpm)	$-33 \pm 5$ ( $P=0.0005$ ) pre-NMDA: $468 \pm 23$	$+1 \pm 17$ ( $P=0.4$ ) pre-NMDA: $477 \pm 57$

Changes in brown adipose tissue (BAT) sympathetic nerve activity (SNA), BAT temperature (T<sub>BAT</sub>), expired CO<sub>2</sub> (Exp CO<sub>2</sub>), mean arterial pressure (MAP), and heart rate (HR) following nano-injections of NMDA (0.2 mmol/L, 60 nL) in the ventral lateral preoptic area (vLPO, n = 4) and in the medial preoptic area (MPA, n = 5) after nano-injections of bicuculline (BIC, 1 mmol/L, 60 nL) in the DMH. BIC was injected into DMH under thermoneutral conditions (Figure 4A,C) in the absence of BAT SNA.

*P* values refer to the differences in physiologic parameters between before and after the nano-injections of NMDA.

TABLE 4

Effect of activating vLPO neurons during the BAT sympathoexcitation evoked by disinhibition and by activation of neurons in rRPa

	<b>NMDA in vLPO after BIC in the rRPa</b>	<b>NMDA in vLPO after NMDA in the rRPa</b>
BAT SNA(%BL)	-15 ± 47 ( <i>P</i> = 0.2) pre-NMDA: 1937 ± 944	-1420 ± 707 ( <i>P</i> = 0.01) pre-NMDA: 1557 ± 704
T <sub>BAT</sub> (°C)	+0.1 ± 0.1 ( <i>P</i> = 0.02) pre-NMDA: 38.2 ± 0.8	-1.0 ± 0.7 ( <i>P</i> = 0.02) pre-NMDA: 38.3 ± 0.4
Exp CO <sub>2</sub> (%)	+0.04 ± 0.1 ( <i>P</i> = 0.2) pre-NMDA: 6.8 ± 1.2	-0.7 ± 0.4 ( <i>P</i> = 0.01) pre-NMDA: 6.5 ± 1.1
T <sub>CORE</sub> (°C)	+0.1 ± 0.01 ( <i>P</i> = 0.0001) pre-NMDA: 38.4 ± 0.8	-0.1 ± 0.1 ( <i>P</i> = 0.1) pre-NMDA: 38.6 ± 0.6
MAP(mmHg)	-6 ± 4 ( <i>P</i> = 0.01) pre-NMDA: 115 ± 17	-13 ± 11 ( <i>P</i> = 0.02) pre-NMDA: 126 ± 17
HR (bpm)	-34 ± 32 ( <i>P</i> = 0.02) pre-NMDA: 446 ± 63	-64 ± 49 ( <i>P</i> = 0.02) pre-NMDA: 426 ± 83

Changes in brown adipose tissue (BAT) sympathetic nerve activity (SNA), BAT temperature T<sub>BAT</sub>, expired CO<sub>2</sub> (Exp CO<sub>2</sub>), mean arterial pressure (MAP), and heart rate (HR) following nano-injections of NMDA (0.2 mmol/L, 60 nL) in the ventral lateral preoptic area (vLPO) following nano-injections of bicuculline (BIC, 1 mmol/L, 60 nL, n = 6) or of NMDA (0.2 mmol/L, 60 nL, n = 5) in the rostral raphe pallidus (rRPa). NMDA and BIC were injected under thermoneutral condition (Figure 5A,C) in the absence of BAT SNA.

*P* values refer to the differences in physiologic parameters between before and after the nano-injections of NMDA in the vLPO.

Effect of glutamate receptor blockade in the DMH or muscimol in the MnPO on the BAT stimulation evoked by inhibition of the vLPO

**TABLE 5**

	<b>AP5/CNQX in DMH after Musc in vLPO</b>	<b>Musc in MnPO after Musc in vLPO</b>
BAT SNA (%BL)	-1259 ± 680 ( <i>P</i> = 0.02) pre-AP5/CNQX: 1378 ± 673	-47 ± 349 ( <i>P</i> = 0.4) pre-Musc in MnPO: 2345 ± 1677
T <sub>BAT</sub> (°C)	-1.3 ± 0.3 ( <i>P</i> = 0.001) pre-AP5/CNQX: 38.2 ± 0.5	+0.1 ± 0.1 ( <i>P</i> = 0.04) pre-Musc in MnPO: 38.7 ± 0.7
Exp CO <sub>2</sub> (%)	-0.8 ± 0.1 ( <i>P</i> = 0.0001) pre-AP5/CNQX: 7.3 ± 1.2	+0.1 ± 0.1 ( <i>P</i> = 0.1) pre-Musc in MnPO: 6.5 ± 1.0
T <sub>CORE</sub> (°C)	-0.2 ± 0.1 ( <i>P</i> = 0.02) pre-AP5/CNQX: 38.5 ± 0.8	+0.1 ± 0.01 ( <i>P</i> = 0.0004) pre-Musc in MnPO: 38.7 ± 0.7
MAP (mmHg)	-12 ± 9 ( <i>P</i> = 0.02) pre-AP5/CNQX: 127 ± 27	-1 ± 2 ( <i>P</i> = 0.2) pre-Musc in MnPO: 123 ± 19
HR (bpm)	-40 ± 19 ( <i>P</i> = 0.01) pre-AP5/CNQX: 449 ± 33	-1 ± 5 ( <i>P</i> = 0.4) pre-Musc in MnPO: 475 ± 40

Changes in brown adipose tissue (BAT) sympathetic nerve activity (SNA), BAT temperature (T<sub>BAT</sub>), expired CO<sub>2</sub> (Exp CO<sub>2</sub>), mean arterial pressure (MAP), and heart rate (HR) following nano-injections of AP5/CNQX (5 mmol/L each, 60 nL) in the DMH (Figure 6A, n = 4) and after nano-injections of muscimol (Musc, 1.2 mmol/L, 60 nL) in the medial preoptic area (MnPO) (Figure 6C, n = 4). AP5/CNQX in DMH and Musc in MnPO were injected during the BAT sympathoexcitatory response to inhibition of vLPO neurons.

*P* values refer to the differences in physiologic parameters between before and after the nano-injections of AP5/CNQX in the DMH, or before and after muscimol in the MnPO.

**TABLE 6**

Neuronal activity in the vLPO controls muscle shivering EMGs

	NMDA in vLPO during shivering evoked by skin cooling	NMDA in vLPO during shivering evoked by PGE <sub>2</sub> in the MPA	Muscimol in the vLPO
Forepaw EMG (%BL)	-149 ± 77 ( <i>P</i> = 0.01) pre-NMDA: 327 ± 220	-910 ± 637 ( <i>P</i> = 0.03) pre-NMDA: 935 ± 630	+531 ± 354 ( <i>P</i> = 0.03) pre-muscimol: 100 ± 1
Nuchal EMG (%BL)	-699 ± 496 ( <i>P</i> = 0.02) pre-NMDA: 724 ± 479	-212 ± 81 ( <i>P</i> = 0.007) pre-NMDA: 255 ± 69	+1715 ± 1101 ( <i>P</i> = 0.03) pre-muscimol: 100 ± 0
Masseter EMG (%BL)	-1330 ± 977 ( <i>P</i> = 0.02) pre-NMDA: 1340 ± 972	-213 ± 137 ( <i>P</i> = 0.03) pre-NMDA: 261 ± 124	+1975 ± 1065 ( <i>P</i> = 0.02) pre-muscimol: 100 ± 0
T <sub>BAT</sub> (°C)	-0.2 ± 0.2 ( <i>P</i> = 0.01) pre-NMDA: 36.4 ± 0.7	-0.2 ± 0.05 ( <i>P</i> = 0.02) pre-NMDA: 5.8 ± 1.1	+3.2 ± 0.6 ( <i>P</i> = 0.001) pre-muscimol: 36.1 ± 0.8
Exp CO <sub>2</sub> (%)	-0.6 ± 0.4 ( <i>P</i> = 0.007) pre-NMDA: 5.7 ± 0.9	-0.1 ± 0.2 ( <i>P</i> = 0.3) pre-NMDA: 38.4 ± 0.2	+1.8 ± 0.8 ( <i>P</i> = 0.01) pre-muscimol: 4.6 ± 0.3
HR (bpm)	-32 ± 12 ( <i>P</i> = 0.001) pre-NMDA: 441 ± 24	-11 ± 5 ( <i>P</i> = 0.03) pre-NMDA: 445 ± 30	+71 ± 32 ( <i>P</i> = 0.01) pre-muscimol: 404 ± 32

Changes in muscle shivering EMGs in the forepaw, nuchal, and masseter muscles, in BAT temperature (T<sub>BAT</sub>), expired CO<sub>2</sub> (Exp CO<sub>2</sub>), and heart rate (HR) following nano-injections of NMDA (0.2 mmol/L, 60 nL) in the ventral lateral preoptic area (vLPO) during skin cooling-evoked shivering (Figure 8B, n = 6), or during shivering evoked by nano-injections of prostaglandin (PGE<sub>2</sub>) in the medial preoptic area (MPA) (Figure 8F, n = 4); and following nano-injections muscimol (1.2 mmol/L, 60 nL) in the vLPO (Figure 8I, n = 4).

*P* values refer to the differences in physiologic parameters between before and after the nano-injections of NMDA in the vLPO and at the peak response to muscimol nano-injections in the vLPO.